ACS MEASUREMENT SCIENCE Au
AN OPEN ACCESS JOURNAL OF THE AMERICAN CHEMICAL SOCIETY

pubs.acs.org/measureau
Review

Advances and Perspectives of Responsive Probes for Measuring γ-Glutamyl Transpeptidase

Published as part of ACS Measurement Science Au virtual special issue "2023 Rising Stars".

Yiming Zhang, Zexi Zhang, Miaomiao Wu, and Run Zhang*

Cite This: *ACS Meas. Sci. Au* 2024, 4, 54–75
Read Online

ABSTRACT: Gamma-glutamyltransferase (GGT) is a plasma-membrane-bound enzyme that is involved in the γ-glutamyl cycle, like metabolism of glutathione (GSH). This enzyme plays an important role in protecting cells from oxidative stress, thus being tested as a key biomarker for several medical conditions, such as liver injury, carcinogenesis, and tumor progression. For measuring GGT activity, a number of bioanalytical methods have emerged, such as chromatography, colorimetric, electrochemical, and luminescence analyses. Among these approaches, probes that can specifically respond to GGT are contributing significantly to measuring its activity in vitro and in vivo. This review thus aims to highlight the recent advances in the development of responsive probes for GGT measurement and their practical applications. Responsive probes for fluorescence analysis, including "off−on", near-infrared (NIR), two-photon, and ratiometric fluorescence response probes, are initially summarized, followed by discussing the advances in the development of other probes, such as bioluminescence, chemiluminescence, photoacoustic, Raman, magnetic resonance imaging (MRI), and positron emission tomography (PET). The practical applications of the responsive probes in cancer diagnosis and treatment monitoring and GGT inhibitor screening are then highlighted. Based on this information, the advantages, challenges, and prospects of responsive probe technology for GGT measurement are analyzed.

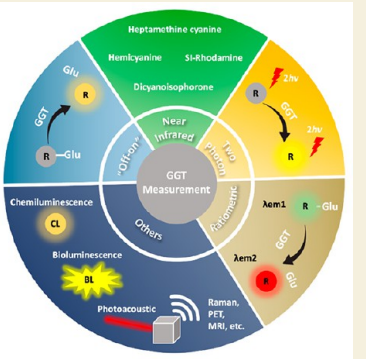

KEYWORDS: *responsive probes, γ-glutamyl transpeptidase, fluorescence measurement, activatable materials, cancer diagnosis and treatment, ratiometric fluorescence probe, near-infrared fluorescence, two-photon fluorescence, photodynamic therapy, glutathione*

1. INTRODUCTION

Enzymes, often termed biological catalysts, constitute a group of proteins that play central roles in a variety of biological processes. These processes encompass crucial functions including digestion, metabolism, nucleic acid replication, and cellular signaling.[1,2] The distinctive functions that enzymes fulfill within these biological contexts render them indispensable agents in maintaining the fundamental operations of cells.[3,4] For example, γ-glutamyltransferase (GGT) is an enzyme residing on the extracellular cell membrane for maintaining cellular homeostasis through the decomposition of glutathione (GSH).[5] Specifically, GGT catalyzes hydrolysis or transpeptidation, facilitating the cleavage and transfer of g-glutamyl groups of GSH and other derivatives.[6] This intricate process involves the transfer of γ-glutamyl residues from disparate g-glutamylated compounds to water and amino acids.[7] The decomposed amino acids are also employed by cells for physiologically defending against oxidative stress.[8] Notably, many research indicate that GGT is involved in free radical generation within specific contexts, particularly in the presence of iron or other transition metals.[9,10] Furthermore, GGT plays a role in the metabolism of leukotriene,[11] a pivotal contributor to inflammatory responses.

GGT in the body has been one of the key biomarkers in both the diagnosis and treatment monitoring of numerous medical conditions.[12] For instance, as a key enzyme in GSH metabolism, GGT's activity is generally tested as an indicator of oxidative stress and liver injury for diagnosis of hepatic and biliary disorders.[13] In liver injury or compromised bile transport, GGT is highly expressed and subsequently a high level of GGT presents in the bloodstream.[14] Thus, measuring GGT activity in liver and blood would contribute to the diagnosis of liver and biliary injury.[15] Elevated GGT levels are commonly associated with liver pathologies such as hepatitis,[16] cholestasis, cirrhosis,[17] hepatocellular carcinoma, and hepatic

Received: August 31, 2023
Revised: November 7, 2023
Accepted: November 7, 2023
Published: December 4, 2023

injuries triggered by acute or chronic alcohol consumption and medication. In clinical practice, GGT measurements are commonly involved in liver function tests, alongside the tests of alanine aminotransferase (ALT), aspartate aminotransferase (AST), and alkaline phosphatase (ALP) levels.[18] Beyond hepatopathology, changes of GGT levels are also implicated in other conditions, such as diabetes, cardiovascular disorders, and certain cancers.[19] For instance, an elevated GGT level in serum has been confirmed in patients of cardiovascular diseases,[20,21] type 2 diabetes,[22] pancreatitis, pancreatic, and ovarian cancers,[23] and metabolic syndrome.[24] Apart from its diagnostic utility, GGT holds promise as a therapeutic target for several diseases. For example, inhibiting GGT activity in animal models of nonalcoholic fatty liver disease (NAFLD) may enhance insulin sensitivity and reduce hepatic fat deposition.[25,26]

Therefore, measurement of GGT activity in the body and biological fluids (e.g., serum) is essential for early diagnosis and treatment monitoring of various diseases. Until now, a series of methods have been developed for measuring GGT, such as high-performance liquid chromatography (HPLC),[27] colorimetric analysis based on *p*-nitroanilide,[28] electrochemical analysis,[29] and luminescence analysis.[6] Of these methods, bioanalysis using responsive probes has been particularly interesting.[30] Therefore, in the past few years, a number of responsive probes have been developed for the GGT activity measurement. In this work, we provide a comprehensive overview of the responsive probes, including fluorescence, bioluminescence, chemiluminescence, photoacoustic, Raman, and other probes, for the measurement of GGT activity and highlight their practical applications in disease diagnosis, treatment monitoring, inhibitor screening, etc. The current limitations and future research directions of the development of responsive probes and their applications are also discussed.

2. MEASURING GGT BY A SMALL-MOLECULE-BASED RESPONSIVE FLUORESCENCE PROBE

Fluorescence analysis using small-molecule-based responsive probes has attracted enormous interest in recent decades, primarily owing to their remarkable attributes such as high sensitivity, specificity, simplicity, rapid response, and exceptional efficiency.[31] As a result, a number of responsive molecular probes have been recently developed for fluorescent measurement of GGT's activity.[32] The design of these probes is generally based on the cleavage of the γ-glutamate in glutathione (GSH) and other γ-glutamyl linkages and subsequent intramolecular displacement of thiolate to form amino-substituted products (Figure 1A). As a result of this specific cleavage reaction, the fluorophores would be released, leading to an "off−on" fluorescence response (Figure 1B). In addition, for some other probes, the molecular structures or intramolecular charge transfer (ICT) processes would be varied, resulting in a shift of the emission band for ratiometric fluorescence measurement of GGT (Figure 1C). In the following section, advances in the development of small-molecule-based responsive probes, including the "off−on" and ratiometric fluorescence response probes for fluorescence measurement of GGT activity, are discussed.

2.1. "Off−On" Fluorescence Response Probes for GGT Measurement

Building on the sensing mechanism of GGT-triggered cleavage reaction, Urano and colleagues developed a fluorescence probe

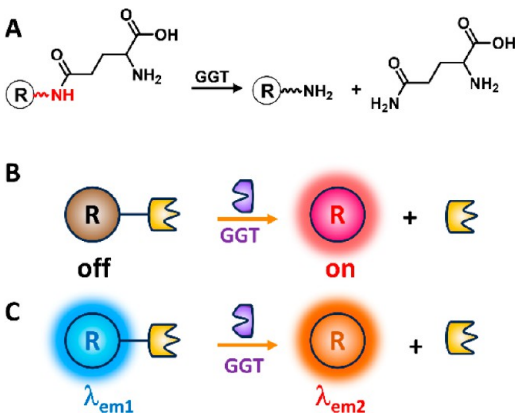

Figure 1. Design of responsive small-molecule probes for fluorescence measurement of GGT based on the specific cleavage of γ-glutamate in GSH and other g-glutamyl linkages (A) and corresponding "off−on" (B) and ratiometric (C) fluorescence responses.

(Figure 2) for GGT and used it for cancer detection (Figure 3).[23] The probe was designed by conjugating the rhodamine green with a γ-glutamyl linker, and the formed γ-glutamyl hydroxymethyl rhodamine green (γGlu-HMRG, Probe #1) showed quenched emission due to the intramolecular spirocyclic caging. The GGT-catalyzed cleavage of the g-glutamyl bond resulted in a greater than 350-fold increase in the green emission.

Although there are advantages of γGlu-HMRG for GGT measurement and the various applications, multiple steps of synthesis procedures with low yield (41%) are required for preparing this probe. Moreover, the probe is also potentially pH sensitive as of the two amino functional groups (-NH_2). To address this issue, Li and co-workers described a one-step reaction to synthesize a chloro-rhodamine (ClR) dye-based probe (CIR-Glu, Probe #2) for GGT measurement (Figure 2).[33] In this probe, the amino group was conjugated with a γ-glutamyl bond, and the closed state of the spiro ring led to the quenching of CIR's emission at 530 nm. In the presence of GGT, the cleavage of the γ-glutamyl bond released the CIR fluorophore, leading to a greater than 400-fold enhancement in fluorescence intensity. This probe showed high sensitivity (Limit of Detection, LOD < 50 mU/L) and selectivity for GGT measurement. Interestingly, the emission of both CIR and CIR-Glu is pH independent, enabling the imaging of GGT activity in HepG2 and LO2 cells.

Except for the sensing mechanism presented in Figure 1, measuring the byproduct of the GGT-catalyzed reaction with glutamlhydrine substrate has also been explored for the design of Rho-GGT (Probe #3) for GGT activity measurement (Figure 4).[34] In a reaction of GGT with glutamlhydrine, a trace amount of hydrazine is produced. The hydrazine could react with the 4-bromobutyriate group of Rho-GGT to release the fluorescent Rho. The probe could be used for measuring GGT in the range 0−100 μM with LOD 0.25 μM. Imaging of GGT activity in live cells and liver injury was then demonstrated.

In another work reported by Li et al., a γ-glutamyl group was incorporated into the cresyl violet (CV) fluorophore to produce the CV-Glu responsive probe (Probe #4) for fluorescence measurement of GGT (Figure 5).[35] The substitution of CV's amino group led to the quenching of the emission, while the GGT-catalyzed cleavage of the γ-glutamyl linker resulted in the recovery of CV's emission at

https://doi.org/10.1021/acsmeasuresciau.3c00045
ACS Meas. Sci. Au 2024, 4, 54−75

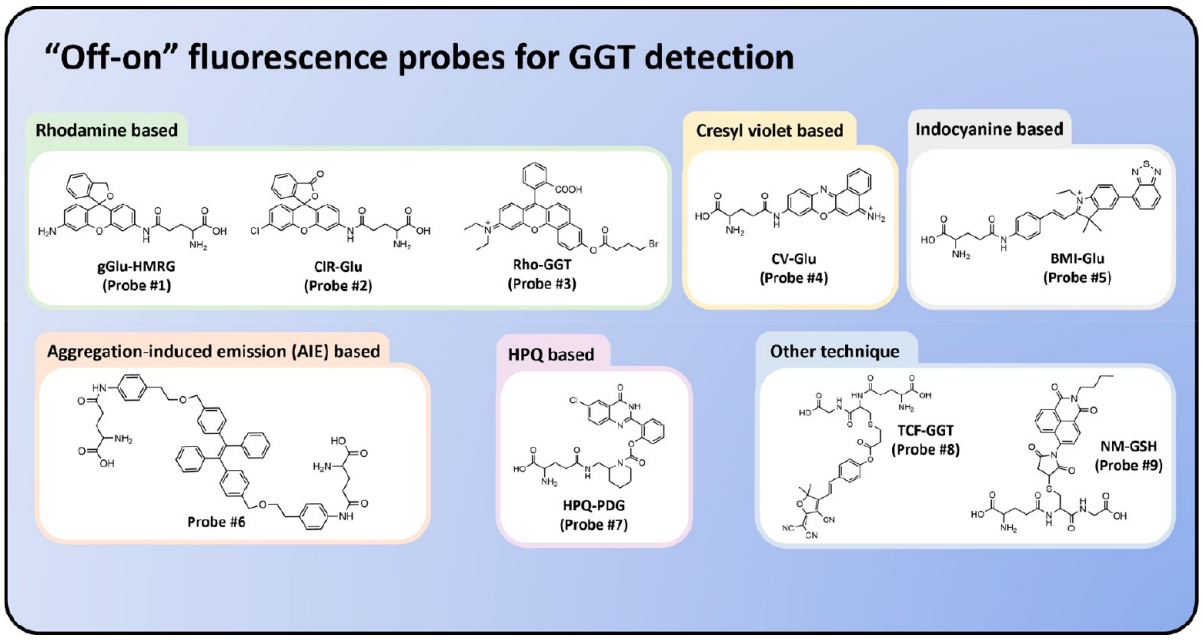

Figure 2. Chemical structure of selected "off−on" responsive probes for the fluorescence measurement of GGT.

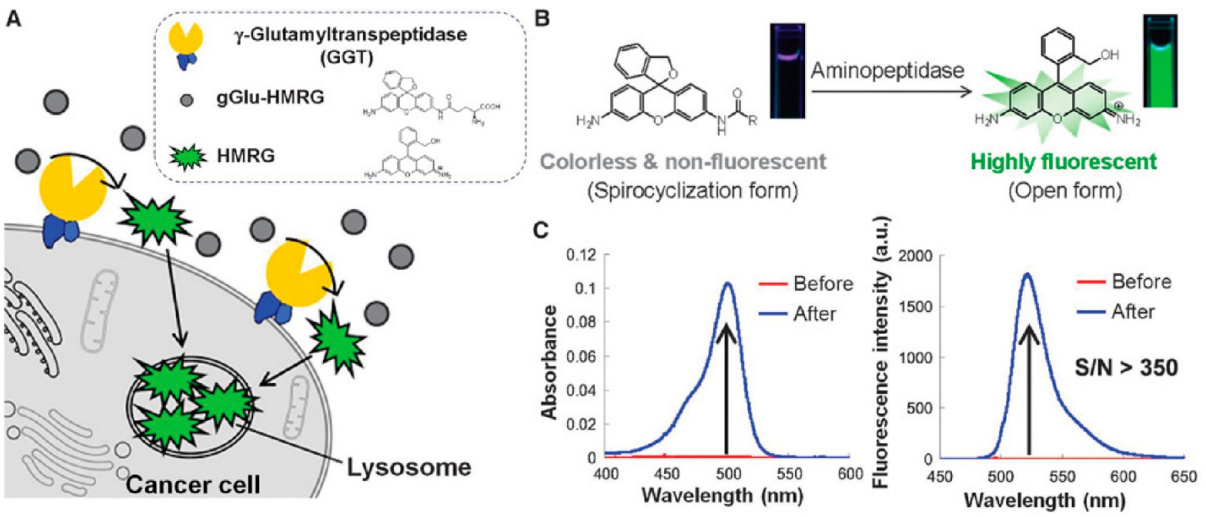

Figure 3. γGlu-HMRG probe for fluorescence measurement of cancer cells' GGT activity. (A) Activation of the γGlu-HMRG probe by GGT on the cancer cell membrane. (B) Molecular structure of γGlu-HMRG (Probe #1) and its sensing reaction to GGT. (C) Changes of absorption and emission spectra of γGlu-HMRG to GGT. Reprinted with permission from ref 23. Copyright 2011 American Association for the Advancement of Science.

615 nm (λ_{ex} = 585 nm). In addition to the enhancement of emission, the color of the test solution changed from light yellow to pink, enabling naked eye analysis of GGT activity. In comparison to γGlu-HMRG and CIR-Glu, the CV-Glu probe showed an even larger enhancement in emission to about 500-fold. Therefore, higher sensitivity was obtained (LOD 5.6 mU/L) for GGT activity analysis in the range of 1−50 U/L. The CV-Glu was then used to measure GGT activity in HepG2 cancer cells and the intracellular GGT level changes upon anticancer drug (NaBu) treatment. In addition to the CV fluorophore, the substituted amino group of indocyanine dye also showed quenched emission because of the interruption of the ICT process. By virtue of this fluorescence quenching mechanism, Guo et al. reported the development of the responsive probe BMI-Glu (Probe #5) for GGT activity measurement (Figure 2).[36] Similarly, a red shift of the absorption spectra from 438 to 512 nm was observed after the cleavage of the γ-glutamyl bond, accompanied by an 8-fold fluorescence enhancement at 578 nm within 25 min of GGT-triggered cleavage reaction. This probe, therefore, showed a relatively lower sensitivity over the probes described above with a LOD of 70.2 mU/L.

One of the key challenges in fluorescence analysis is the quenched emission at high concentration of fluorophore, a well-known phenomenon of "concentration quenching" or "aggregation-caused quenching" (ACQ).[37] Tang's group revealed that the emission could be enhanced upon aggregation for some fluorogens due to the aggregation-induced emission (AIE) and then defined these fluorogens as AIEgens. In sharp contrast to ACQ, AIEgens, like tetraphenylethylene (TPE) derivatives, display significant enhancement in emission upon aggregation. As a result, AIEgens have been

https://doi.org/10.1021/acsmeasuresciau.3c00045
ACS Meas. Sci. Au 2024, 4, 54−75

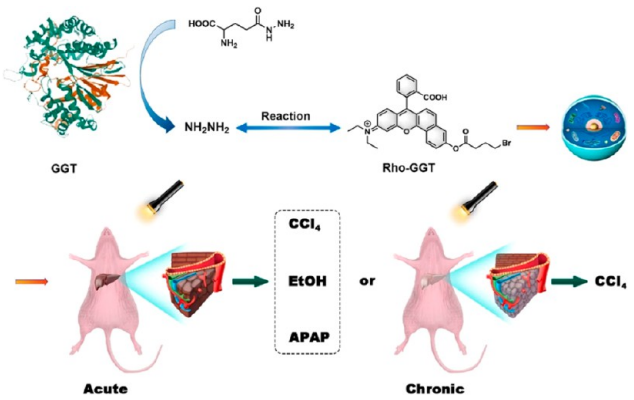

Figure 4. Schematic illustration of the design of the GGT probe (Rho-GGT, Probe #3) for GGT measurement in live cells and liver injury. Reprinted with permission from ref 34. Copyright 2023 Elsevier.

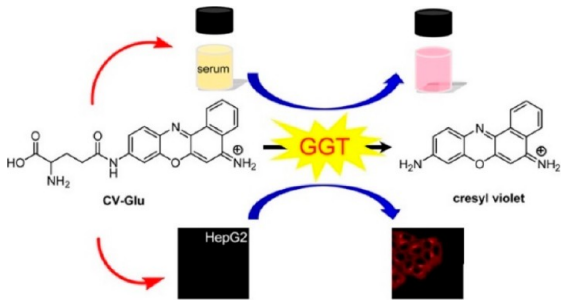

Figure 5. Sensing reaction of CV-Glu (Probe #4) with GGT, color, and fluorescence changes after the sensing reaction and the imaging of GGT in HepG2 cells. Reprinted with permission from ref 35. Copyright 2015 American Chemical Society.

widely used in fluorescence biosensing and imaging, disease diagnosis and treatment, etc. The design of AIE-based responsive probes for biosensing and imaging mainly relies on the modification of their water solubility.[38] In 2016, Hou et al. reported the development of a TPE derivative as the responsive AIEgen for measuring of GGT activity (Figure 6).[39] In this probe (Probe #6), the coupling of hydrophilic g-glutamyl amide groups onto the TPE derivative facilitated the good water solution of the probe. In the presence of GGT, the cleavage of the γ-glutamyl bond resulted in the release of TPE derivative, which has poor water solubility. The aggregation of TPE derivative in aqueous solution then led to the enhancement of the emission at 472 nm (λ_{ex} = 360 nm). This probe is able to measure the GGT activity at lower concentration (LOD 0.59 U/L) in PBS buffer with 20 μM CTAB, and GGT in human serum and A2780 cells.

In addition to the cleavage of primary aromatic-amine-based γ-glutamyl linkages, the cleavage of aliphatic-amine-based γ-glutamyl linkages, like the derivatives of GSH, has also been explored as the recognition unit for the development of responsive probes for GGT. For example, Ou-Yang and colleagues reported the development of a precipitating fluorochrome (2-(2-hydroxyl-phenyl)-6-chloro-4-(3*H*)-quinazo-linone (HPQ))-based probe (HPQ-PDG, Probe #7) for GGT measurement in 2018 (Figure 7).[40] In this probe, the GGT recognition unit, γ-glutamyl, was conjugated to the HPQ through a tertiary carbamyl linkage. The restriction of the excited-state intramolecular proton transfer (ESIPT) process together with the improvement of the water solubility of HPQ contributed to the quenched emission of probe HPQ-PDG. In the presence of GGT, the cleavage of γ-glutamyl was followed by 1,2-diamine-based cyclization and release of HPQ, which has poor water solubility. Similar to AIEgens,[39] the solid-state fluorescence of HPQ was observed, enabling a 53-fold increase in emission at 500 nm (λ_{ex} = 370 nm) for GGT measurement in the range of 0.05−80 U/L (LOD 16.7 mU/L). The practical application of the HPQ-PDG probe was then demonstrated in GGT activity measurement in mice serum, fluorescence imaging in living cells, and HCT116 tumor tissue slice.

Cleavage of γ-glutamyl from GSH has also been employed for the design of responsive probes for GGT measurement. These probes, such as TCF-GGT (Probe #8)[41] and NM-GSH (Probe #9) (Figure 2),[42] were developed by attaching GSH to fluorophores, such as dicyanomethyldifuranyl (TCF-OH) and 1,8-naphthalimide,[43] respectively, through the thioether. The GGT-catalyzed cleavage of γ-glutamyl from GSH triggered an intramolecular cyclization and elimination cascade reaction. The release (TCH-OH) and structural modification of the fluorophore (naphthalimide derivative) then led to the enhancement of emission at 605 and 473 nm for probes TCF-GGT and NM-GSH, respectively. In comparison with probe NM-GSH, TCH-GGT exhibited higher sensitivity (LOD 41 mU/L) and long excitation and emission wavelengths ($\lambda_{ex/em}$ = 520/605 nm), enabling it to be used for fluorescence imaging of GGT activity in tumor-bearing mice.

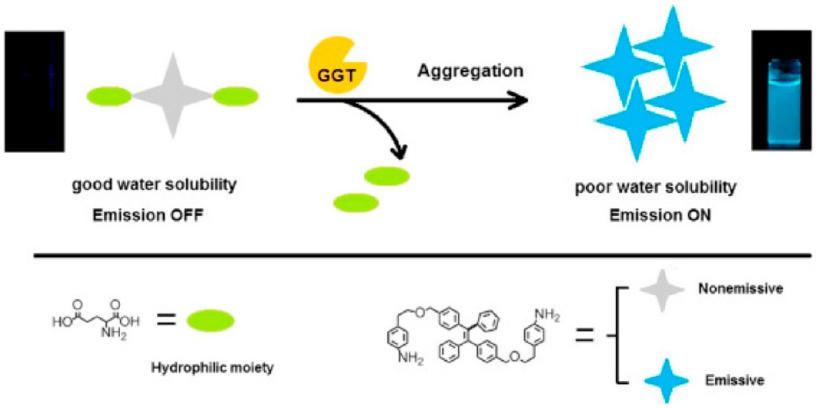

Figure 6. Design of the TPE-based AIE probe (Probe #6) for measurement of GGT, the sensing mechanism, and the change of fluorescence. Reprinted with permission from ref 39. Copyright 2016 Elsevier.

https://doi.org/10.1021/acsmeasuresciau.3c00045
ACS Meas. Sci. Au 2024, 4, 54−75

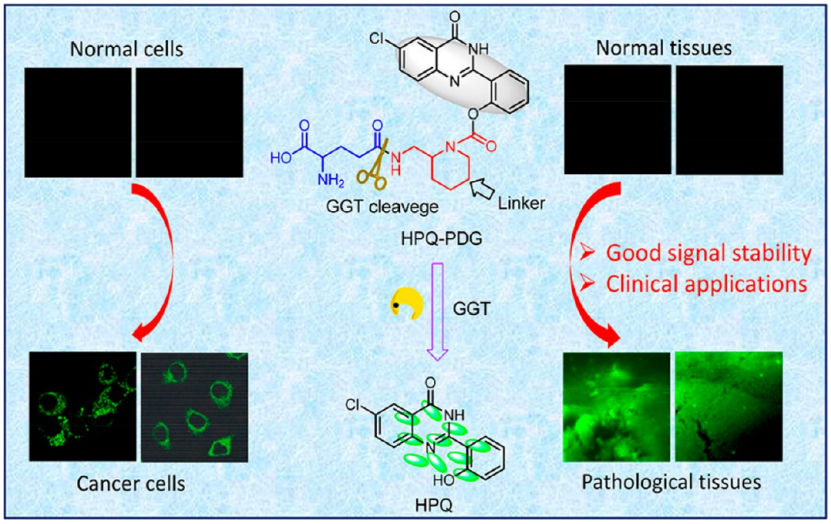

Figure 7. Sensing mechanism of HPQ-PDG (Probe #7) to GGT and fluorescence images of GGT in normal/cancer cells and tissues. Reprinted with permission from ref 40. Copyright 2018 American Chemical Society.

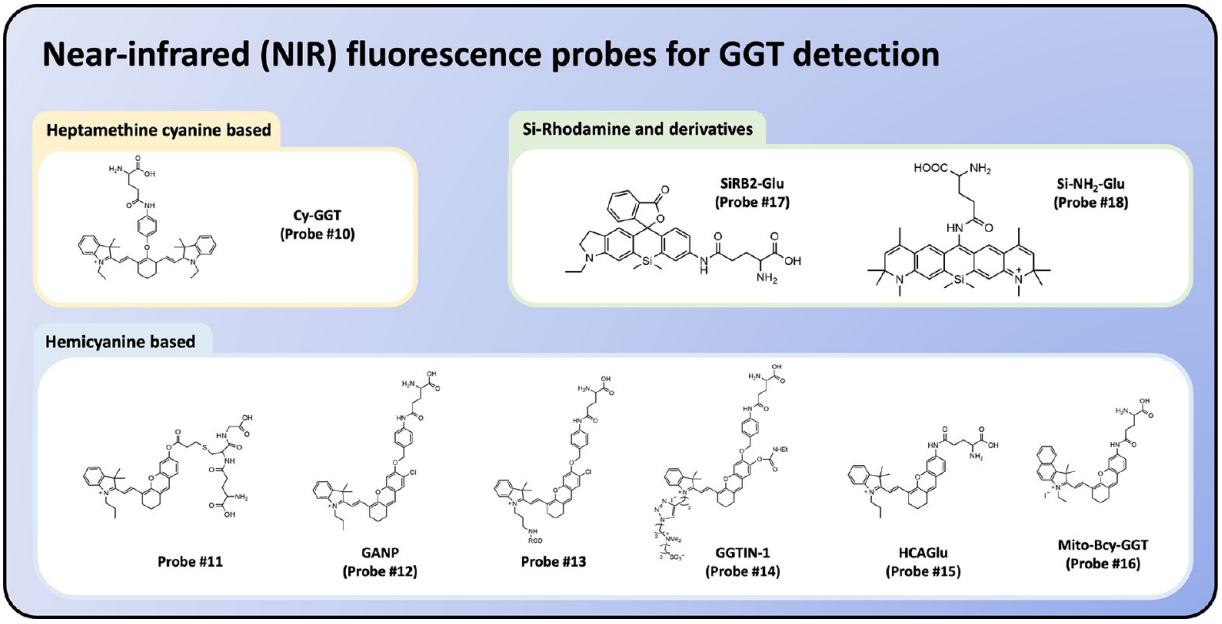

Figure 8. Chemical structure of selected NIR fluorescence probes for GGT.

2.2. Near-Infrared (NIR) Fluorescence Probe for GGT Measurement

One of the primary challenges in fluorescence sensing and imaging is the potential interference caused by background autofluorescence originating from the samples themselves.[44] In the case of biological samples, such as living cells, tissues, and biological fluids (e.g., blood and urine), the predominant source of autofluorescence usually arises from endogenous proteins and other biomolecules. These biomolecules typically emit within the UV−visible range, rendering NIR fluorescence probes more suitable for accurately measuring biomolecules such as GGT in biological samples. Moreover, the NIR fluorescence has higher tissue penetration depth than that of the UV−vis fluorescence,[45] allowing the responsive NIR fluorescence probes for biomolecules' measurement in diseased tissues in vivo. Therefore, the development of NIR fluorescence probes for measuring GGT activity in vitro and in vivo has emerged in recent years. The conjugation of γ-glutamate in GSH and other γ-glutamyl linkages with NIR fluorophores, such as heptamethine cyanine, hemicyanine, Si-rhodamine and derivatives, and dicyanoisophorone,[46] have been the key approaches for the design of these responsive probes (Figure 8).

Through grafting a glutamic acid moiety onto heptamethine cyanine dye, He et al. reported the development of a responsive probe for NIR fluorescence measurement of GGT in aqueous solution, living cells, and pulmonary fibrosis mice (Figures 8 and 9).[47] After the glutamic acid conjugation, the capability of the electron-donating amine was blocked, resulting in weakened emission from the probe Cy-GGT (Probe #10). While in the presence of GGT, the cleavage of the γ-glutamyl linkage led to the release of Cy dyes. The "off−on" fluorescence response at 780 nm was then recorded for GGT analysis. The Cy-GGT showed a fast response (second-order rate constant k_2 = 1.09 × 10^7 M^{-1} s^{-1}), high specificity, and sensitivity (LOD 7.6 mU/L) for GGT measurement in

https://doi.org/10.1021/acsmeasuresciau.3c00045
ACS Meas. Sci. Au 2024, 4, 54−75

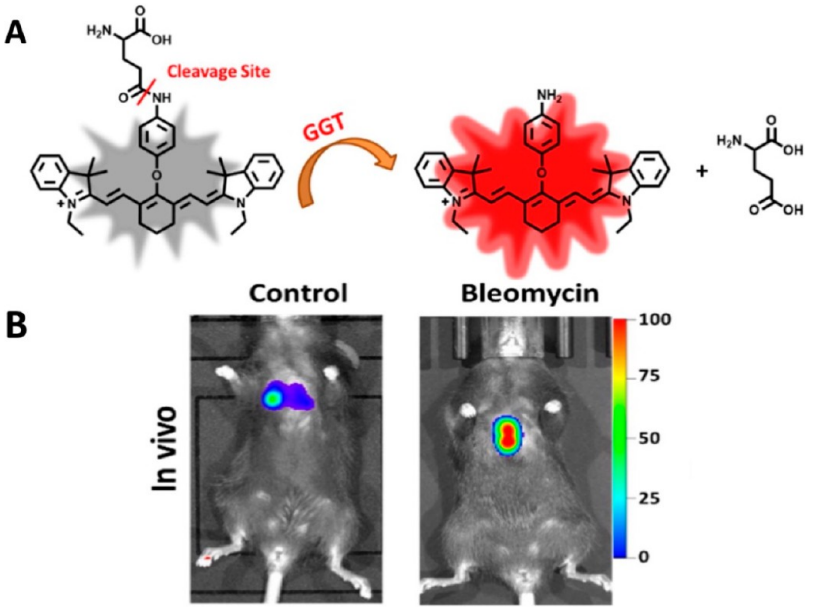

Figure 9. (A) Mechanism for Cy-GGT (Probe #10) for the measurement of GGT. (B) Imaging of GGT in pulmonary fibrosis mice using Cy-GGT. Reprinted with permission from ref 47. Copyright 2020 Elsevier.

HEPES buffer of pH 7.4. Further applications of this probe for GGT activity analysis in RLE-6TN cells and pulmonary fibrosis mice were then demonstrated.

The cyanine dyes, such as IR-780, could react with resorcinol to form a new NIR fluorophore HXPI and derivatives. Similar to resorufin,[48] substitution ("protection") of the hydroxy group of HXPI derivatives could block the ICT process to quench the emission of the probes, while the deprotection of the probes' substituent groups allows for the recovery of the ICT for fluorescence "off–on" response to analytes. On the basis of this sensing mechanism, Li et al. modified the HPXI with GSH through an acrylyl linker to develop a responsive probe (Probe #11) for NIR fluorescence measurement of GGT (Figure 8).[49] Probe #11 showed fluorescence silence due to the restriction of the ICT process. Similar to probe TCF-GGT,[41] the GGT catalyzed the cleavage of g-glutamyl from GSH, which was followed by an intramolecular cyclization and elimination cascade reaction to release HPXI. As a result, the absorption band at 590 nm was red-shifted to 660 nm with the color changed from purple to blue. The NIR emission at 708 nm was then remarkably enhanced for the fluorescence measurement of GGT activity in the range of 1–75 U/L (LOD 0.5 U/L).

The substitution of HPXI with an electron-withdrawing group, like chlorine atom to form mCy-Cl, would be able to adjust HPXI's pK_a (to about 4.5), thus ensuring the high NIR emission under acidic conditions, such as the tumor microenvironment and lysosomes of cancer cells.[50] In another example of a responsive NIR fluorescence probe for GGT measurement, Luo et al. modified the mCy-Cl with glutamic acid through a self-immolative linker *p*-aminobenzyl alcohol to prepare the GGT-responsive probe, GANP (Probe #12) (Figures 8 and 10).[51] The GANP probe presented an about 100-fold enhancement in fluorescence at 720 nm (λ_{ex} = 680 nm) after the GGT-catalyzed cleavage of the γ-glutamyl linkage. GANP showed high sensitivity to GGT (LOD 3.6 mU/L), enabling it to be further used for imaging of GGT activity in OVCAR5 cells and HCT116-tumor-bearing mice

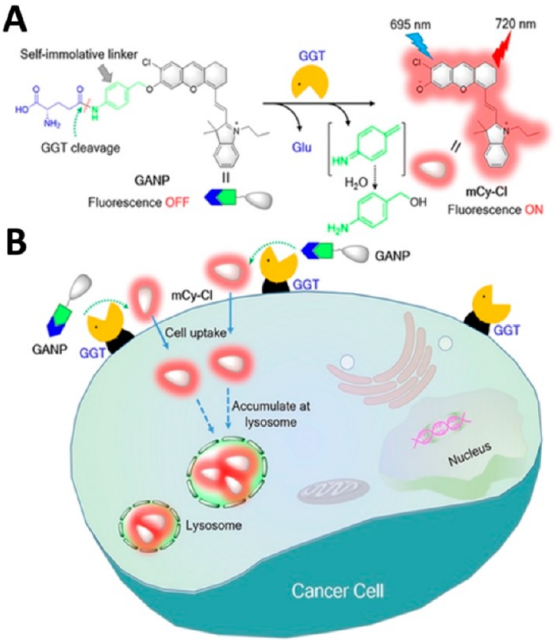

Figure 10. Sensing mechanism of NIR fluorescence probe GANP (Probe #12) for the measurement of GGT. (A) Chemical structure of GANP and GGT-catalyzed reaction. (B) Response of GANP to GGT on the membrane of cancer cells. Reprinted with permission from ref 51. Copyright 2017 Wiley-VCH.

and GGT inhibitor analysis. In a follow-up study by the same research group, $\alpha_v\beta_3$-integrin-receptor-targetable ligand, c-RGD, was integrated into the probe GANP to develop a new probe (Probe #13) for tumor-targeted GGT measurement (Figure 8).[52] As a result of the RGD targeting, Probe #13 could be captured by U87MG tumor cells via $\alpha_v\beta_3$-receptor-mediated endocytosis, allowing for GGT measurement specifically at the tumor site.

GGT is an enzyme that is localized to the cell membrane, with its active site facing the extracellular space.[14] Taking this

https://doi.org/10.1021/acsmeasuresciau.3c00045
ACS Meas. Sci. Au 2024, 4, 54–75

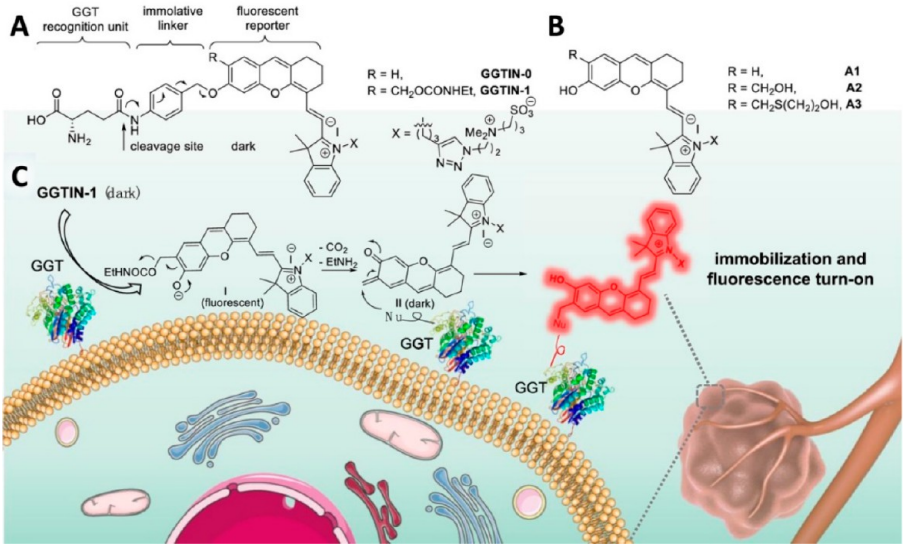

Figure 11. Design of GGTIN-1 (Probe #14) for GGT measurement. (A) Chemical structures of GGTIN-0 and GGTIN-1. (B) Hydrolysates of GGTIN-1 or GGTIN-0 after reaction with GGT. (C) Mechanism of the response of GGTIN-1 to GGT and the subsequent immobilization on the cell membrane after the GGT-triggered reaction. Reprinted with permission with ref 53. Copyright 2020 American Chemical Society.

fact into consideration, Li and colleagues replaced the chlorine atom with an ethylcarbamate on NIR emissive HD dye to develop probe GGTIN-1 (Probe #14) for in situ GGT measurement in vitro and in vivo (Figure 11).[53] In this responsive probe, γ-glutamyl served as the GGT recognition moiety. The cleavage of this linker led to the conversion of ethylcarbamate into highly reactive quinone methide that can further react with nucleophilic residues, such as thiols, hydroxyl, and amine from GGT and/or other proteins nearby, resulting in the measurement of GGT activity at the site of interest. Similar to the above hemicyanine-based responsive probes, the GGTIN-1 showed a sensitive and specific NIR fluorescence response to GGT at 714 nm upon excitation at 687 nm. More interestingly, Probe #15 allowed the fluorescence measurement of GGT at the outer surface of HepG2 cells.

In addition to the hydroxyl derivatives of HPXI, the reaction of IR-780 with 3-nitrophenol and the following of the reduction nitro (-NO_2) to amine (-NH_2) afforded the amine functionalized NIR fluorophore HCA. Then, the conjugation of glutamic acid to HCA through a γ-glutamyl linker allowed Li et al. to prepare the probe HCAGlu (Probe #15) for GGT measurement (Figure 8).[54] The applications of HCAGlu for GGT imaging of HeLa cells and tumor tissues and the in vivo HepG2 bearing tumor model were then demonstrated. In another study by Liu and colleagues, glutamic acid was incorporated into a similar NIR fluorophore, Bcy-NH_2, to produce the probe Mito-Bcy-GGT (Probe #16) for GGT measurement (Figure 8).[55] The sensing mechanism is similar to the probe HCAGlu,[54] while, more interestingly, Probe #16 is able to accumulate in mitochondria due to the cationic and hydrophobic properties of the benzoleindolium moiety, thus allowing it for fluorescence measurement of mitochondrial GGT.

It has been well-known that the replacement of "O" with a "Si" atom would render the rhodamine derivatives with NIR emission,[56] and thus, a series of responsive probes for NIR fluorescence sensing and imaging have been reported,[56−58] including those probes for GGT measurement. For instance, Li et al. modified the amine of SiRB2 with glutamic acid to produce a SiRB2-Glu probe for NIR fluorescence measurement of GGT (Figure 8).[59] The SiRB2-Glu (Probe #17) with closed spirocyclized form showed low NIR fluorescence, while, in the presence of GGT, an "off−on" fluorescence response was clearly observed within 30 min, which allowed it for NIR fluorescence imaging of GGT in colon cancer. Another example of a *meso*-amine Si-rhodamine fluorophore-based responsive probe for GGT measurement represented an interesting "AND" logic gate approach (Figure 12).[60] In this

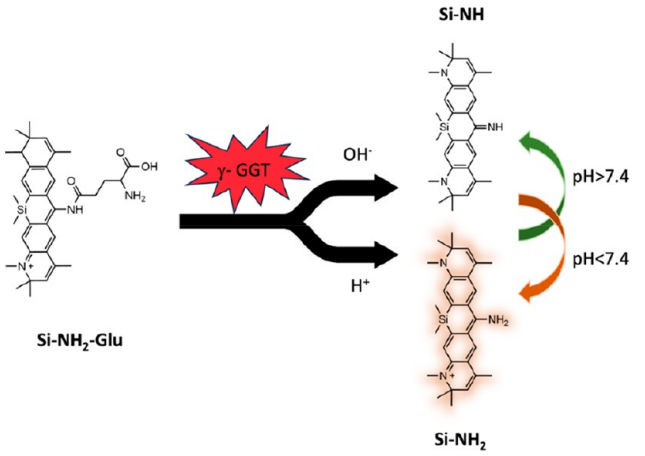

Figure 12. Chemical structure of Si-NH_2-Glu (Probe #18) and its reaction mechanism with GGT.[60]

probe (Si-NH_2-Glu, Probe #18), glutamic acid was incorporated into the Si-NH_2 fluorophore through the typical γ-glutamyl linker. Interestingly, the NIR emission at 654 nm (λ_{ex} = 515 nm) could be observed after GGT-catalyzed cleavage of γ-glutamyl linker at pH < 7.4. This was attributed to the quenching of NIR emission of the deprotonated amine in alkaline solution. The Si-NH_2-Glu with high sensitivity (LOD 51.4 mU/L) was then employed for imaging of GGT in cancer cells and 4T-1-tumor-bearing mice.

https://doi.org/10.1021/acsmeasuresciau.3c00045
ACS Meas. Sci. Au 2024, 4, 54−75

2.3. Responsive Probes for Two-Photon Fluorescence Measurement of GGT

The NIR fluorescence responsive probe provides an effective approach for bioassay in situ in the body with low phototoxicity and bleaching, high tissue penetration depth, and minimal background autofluorescence. As an alternative technique, two-photon fluorescence probes that could be activated by the light source of two NIR photons have also been widely adopted in bioassay and imaging in recent years.[61−63] The excitation by two NIR photons shows high tissue penetration depth with low phototoxicity and bleaching, allowing the responsive probes for high spatiotemporal resolution imaging of biomolecules in situ.[63]

Through incorporating a γ-glutamyl linker into the two-photon excitable fluorophores, responsive probes for two-photon fluorescence measurement of GGT have also been developed in the past few years (Figure 13). For example, due

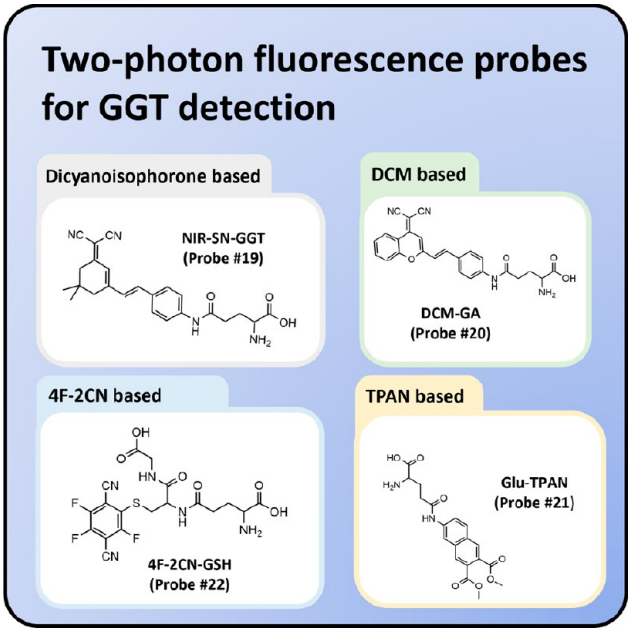

Figure 13. Chemical structure of selected two-photon fluorescence probes for GGT.

to its intense emission at about 650 nm (λ_{ex} = 445 nm), dicyanoisophorone dye (NIR-SN-NH_2) has been explored as the NIR fluorophore for the development of a GGT responsive probe (NIR-SN-GGT, Probe #19) by Li and co-workers (Figure 13).[46] The design of NIR-SN-GGT is similar to the probe TCF-GGT (Probe #8),[41] in which the glutamic acid was directly conjugated to the amine group of NIR-SN-NH_2. This probe responds to GGT in the range of 0−10 mU/L with LOD 24 mU/L. Despite NIR emission, the excitation of NIR-SN-NH_2 located in the UV−vis range (λ_{ex} = 445 nm), which has high light toxicity and low tissue penetration depth. To address this issue, two-photon fluorescence imaging was involved in the evaluation of GGT in tumor cells, tissue, and in vivo tumor bearing mice model. In another study, Zhang et al. modified the -NH_2 of dicyanomethylene-4*H*-pyran (DCM) fluorophore with g-glutamyl linker to develop a two-photon fluorescence "off−on" response probe (DCM-GA, Probe #20) for GGT measurement (Figure 14).[13] Similar to NIR-SN-GGT, the ICT process was restricted due to the γ-glutamyl functionalization; thus, the emission of DCM-GA at 635 nm was weakened. The DCM-GA showed a large two-photon cross section ($\Phi\delta$ = 150 GM) with excitation at 820 nm, allowing it to be used for two-photon fluorescence imaging of GGT in living A2780 cells and zebrafish.

TPAN (6-naphthylamine-2,3-dicarboxylate) is another fluorophore that can be excited by two-photon NIR light (λ_{ex} = 720 nm) with strong green fluorescence at 490 nm. By conjugating the -NH_2 of TPAN with glutamic acid, the emission of Glu-TPAN (Probe #21) (Figure 13) was quenched due to the restriction of the ICT process.[64] This Glu-TPAN probe allowed for one-photon fluorescence measurement of GGT in the range of 0.2−5 U/L and LOD 147 mU/L and two-photon fluorescence imaging of GGT in HepG2 and L02 cells and *C. elegans* and zebrafish. In another study, Huo et al. described a cascade-reaction-based two-photon fluorescence probe (Figure 13) for GGT measurement.[65] The probe, 4F-2CN-GSH (Probe #22), was developed by conjugating GSH to 4F-2CN through a thioether bond. Interestingly, the GGT-triggered cleavage of the γ-glutamyl linker led to a subsequent cyclization. The blue emission of 4F-2CN-GSH was red-shifted to blue-green, and the intensity at 490 nm increased over time. The probe showed two-photon excitation at 780−900 nm and a large cross section of 63 GM upon excitation at 850 nm. Using 4F-2CN-GSH as a tool, two-photon fluorescence imaging of GGT activity of OVCAR3, SKOV3, and HUVEC cells was then demonstrated.

2.4. Responsive Probes for Ratiometric Fluorescence Measurement of GGT

Despite that the above "off−on" fluorescence response probes have been successfully applied for GGT measurement in vitro and in vivo, it remains challenging for quantitative determination of GGT activity in practical samples because of the interference caused by various factors, such as autofluorescence, excitation source fluctuation, local concentration of probes, light scattering, etc.[66,67] Through introducing another emission peak as the reference, the fabricated dual emission

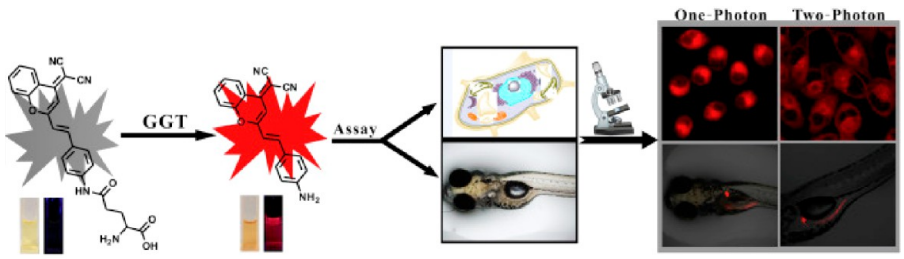

Figure 14. Chemical structure of DCM-GA (Probe #20) and its response with GGT in living cells and zebrafish by one- and two-photon imaging. Reprinted with permission from ref 13. Copyright 2016 Elsevier.

https://doi.org/10.1021/acsmeasuresciau.3c00045
ACS Meas. Sci. Au 2024, 4, 54−75

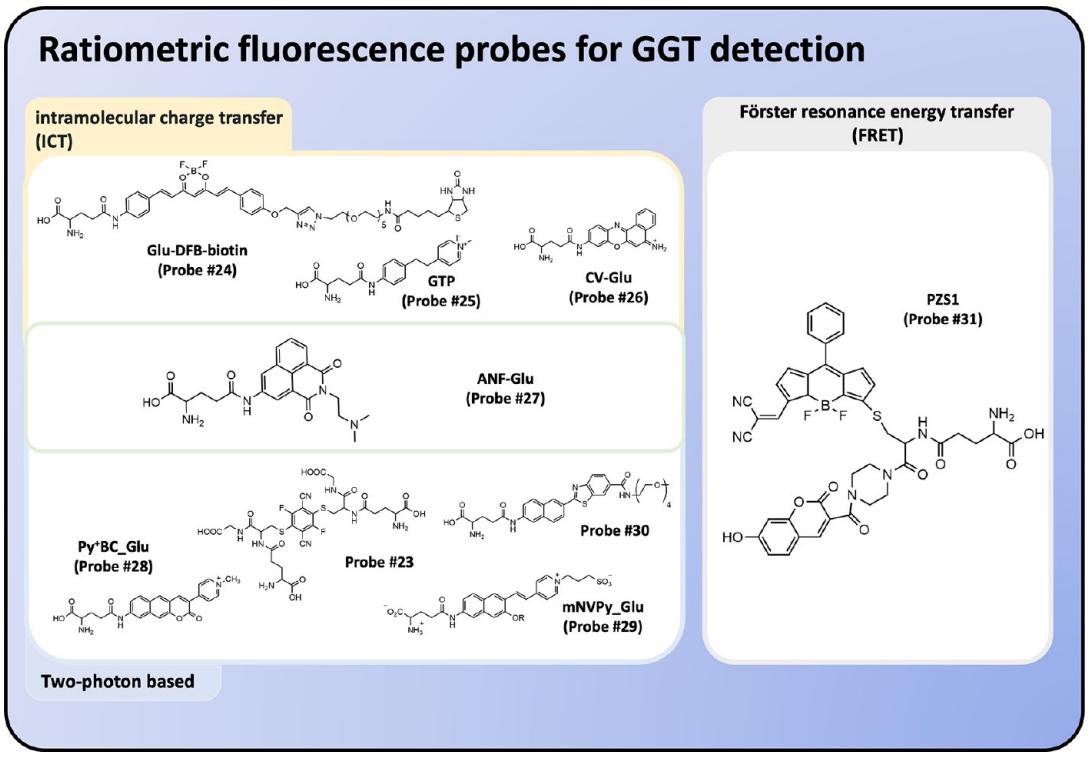

Figure 15. Chemical structure of selected ratiometric fluorescence probes for GGT.

probes and/or ratiometric fluorescence probes would be an effective solution for quantitative measurement of GGT. In contrast to the "off−on" fluorescence response probes, the ratiometric fluorescence probes introduced an "internal standard" for self-calibration when quantitative fluorescence measurement is required, and therefore, the more reliable data would be obtained for fluorescence bioassay and imaging.[68] The structures of several typical ratiometric fluorescence probes, including the ratiometric two-photon fluorescence probes, are highlighted in Figure 15.

By using a fluorophore similar to Probe #22, Wang and colleagues described the design and preparation of Probe #23 for GGT measurement in blood serum and living cells (Figure 15).[69] Probe #23 showed a similar sensing mechanism with Probe #22, while a blue shift of the emission spectra from 494 to 452 nm was noticed, resulting in a ratiometric fluorescence response to GGT. Incorporating γ-glutamyl and biotin (cancer cell targeting ligand) into curcuminoid difluoroboron fluorophore, Bai et al. reported the development of a dual emission NIR fluorescence probe (Figure 15) for GGT measurement (Figure 16).[70] The probe Glu-DFB-biotin (Probe #24) showed green emission at 565 nm, while the fluorescence peak shifted to 670 nm in the presence of GGT. This red shift of the emission peak was attributed to the restriction and recovery of the ICT process. The decrease of emission at 565 nm and the increase of the emission at 670 nm potentially facilitate the Glu-DFB-biotin for ratiometric fluorescence measurement of GGT. Although the ratiometric fluorescence responses in aqueous solution were not presented, corresponding measurements in living QSG-7701, HepG2, and HeLa cells were demonstrated using Glu-DFB-biotin as the GGT probe.

Similar ICT-mechanism-based ratiometric fluorescence probes have been developed by the incorporation of γ-glutamyl into fluorophores, including (*E*)-4-(4-aminostyryl)-1-methylpyridin-1-ium iodide and cresyl violet (CV) for the fabrication of responsive probes (GTP, Probe #25) (Figure 15)[71] and CV-Glu (Probe #26) (Figure 15),[72] respectively, for ratiometric fluorescence measurement of GGT. For the probe GTP, the emission at 500 nm decreased while emission at 560 nm increased upon the GGT-catalyzed cleavage of γ-glutamyl linker. For the CV-Glu probe, the cleavage of the γ-glutamyl linker induced the decrease of emission at 580 nm and increase of emission at 625 nm. The ratio ($I_{625/580}$) was increased from 0.77 to 10.3, allowing the CV-Glu for ratiometric fluorescence analysis of GGT in living cells and colon cancer in a mouse model.

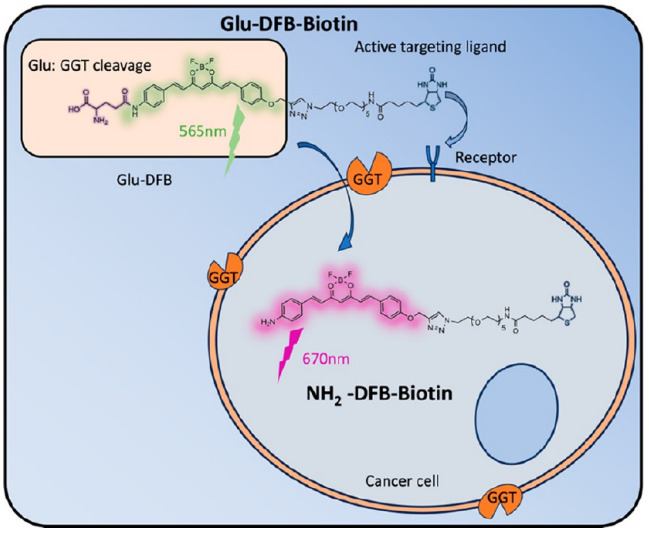

Figure 16. Curcuminoid-difluoroboron-based tumor-targeting dual-channel fluorescent probe Glu-DFB-biotin (Probe #24) for GGT measurement in cancer cells.[70]

https://doi.org/10.1021/acsmeasuresciau.3c00045
ACS Meas. Sci. Au 2024, 4, 54−75

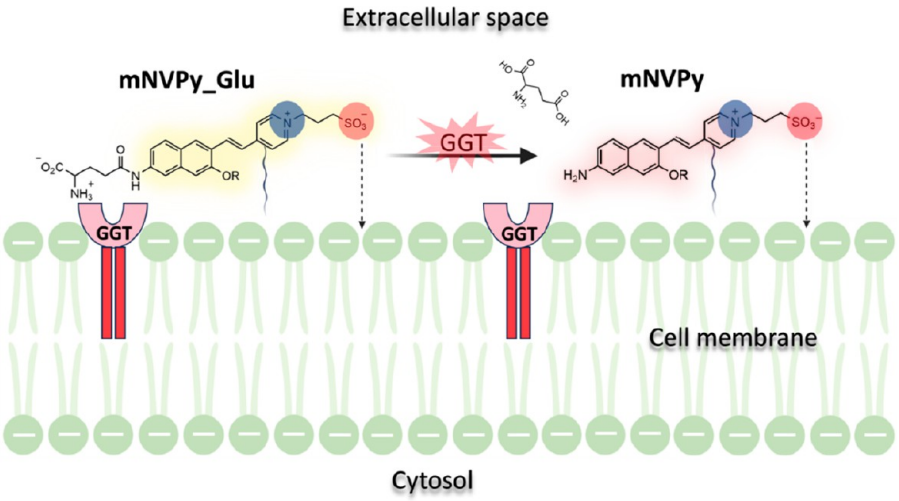

Figure 17. Sensing mechanism of mNVPy_Glu (Probe #29) for the measurement of GGT.[75]

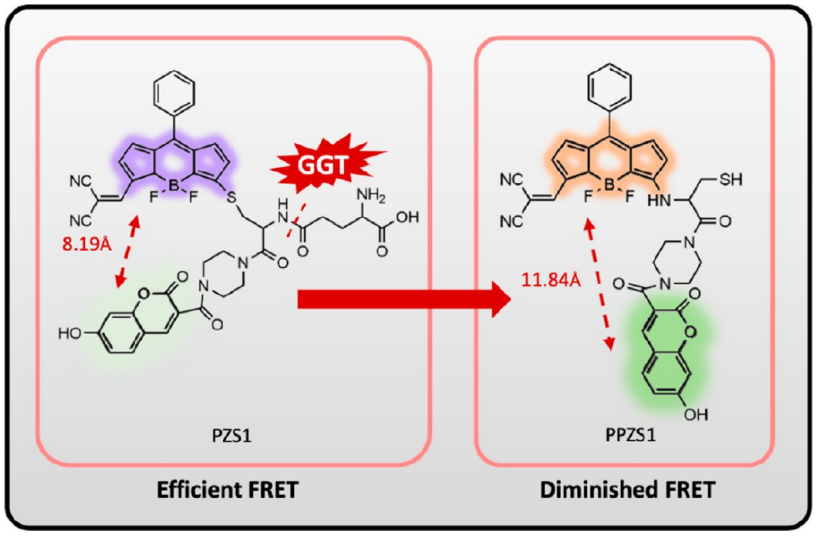

Figure 18. Chemical structure and mechanism of FRET-based ratiometric probe PZS1 (Probe #31) for two-photon fluorescence measurement of GGT.[78]

Taking advantage of the two-photon fluorescence bioassay and imaging technique, several probes for the two-photon ratiometric fluorescence measurement of GGT activity have been developed. For instance, by exploring the ICT mechanism of naphthalimide fluorophore,[43] Zhang et al. synthesized a probe ANF-Glu (Probe #27) for GGT measurement (Figure 15).[73] The probe ANF-Glu was developed by directly conjugating glutamic acid to -NH_2 functionalized naphthalimide dye through a γ-glutamyl linker. Similar to other GGT-responsive probes, the cleavage of the γ-glutamyl linker led to the changes of the ICT process. The fluorescence peak at 441 nm was diminished, and a new emission centered at 531 nm emerged, accompanied by the fluorescence color changes from blue to green. Interestingly, after cleavage of the γ-glutamyl linker, the production of ANF with a -NH_2 functional group can further respond to *N*-acetyltransferase (NAT), an enzyme highly expressed in the DNA damage area. Therefore, this ANF-Glu probe was claimed to determine the DNA damage (by measuring NAT) in cancer cells (by measuring GGT).

In 2019, Reo et al. reported the development of a benzocoumarin-based two-photon fluorescent probe for GGT measurement.[74] The probe (Py^+BC_Glu, Probe #28) was developed by incorporating GGT-cleavable γ-glutamyl onto the Py^+BC fluorophore. This probe showed a 70 nm red-shift emission from 570 to 640 nm after cleavage of the γ-glutamyl. The two-photon cross section was 133 GM at 840 nm for Py^+BC_Glu and 195 GM at 870 nm for Py^+BC, allowing for two-photon ratiometric fluorescence measurement of GGT in HeLa cancer cells and CT-26 tumor bearing mice. In a follow-up study by the same research group, GGT-responsive γ-glutamyl linker was conjugated to -NH_2 of a naphthalene derived fluorophore, mNVPy.[75] More importantly, considering the nature of cell membrane localization of GGT, one long alkyl chain with zwitterionic character was conjugated to the other end of mNVPy, facilitating mNVPy cell membrane staining properties.[76] The mNVPy_Glu (Probe #29) (Figures 15 and 17), therefore, could respond to membrane localized GGT with high potential for quantitative measurement of GGT activity, similar to the probe GGTIN-1.[53] Similar to the probe Py^+BC_Glu, the emission at 544 nm was decreased and

https://doi.org/10.1021/acsmeasuresciau.3c00045
ACS Meas. Sci. Au 2024, 4, 54−75

the emission at 610 nm was increased upon the GGT-catalyzed cleavage of the γ-glutamyl linker. The two-photon cross section was 115 GM at 810 nm for mNVPy_Glu and 119 GM at 900 nm for mNVPy. As a result of the cell membrane staining characteristic, the mNVPy_Glu demonstrated its capability for two-photon ratiometric fluorescence imaging of GGT on membranes in cancer cells and tissues. Kim and colleagues also described the preparation of a two-photon probe (Probe #30) (Figure 15) for ratiometric fluorescence measurement of GGT in colon cancer tissues by integrating the naphthalene derived fluorophore with a g-glutamyl linker.[77] The introduction of the ethylene glycol allowed the probe to have high water solubility for ratiometric ($I_{527/456}$) to one-photon fluorescence imaging of GGT in colon cancer.

In addition to the ICT mechanism, the Förster resonance energy transfer (FRET) has been well-known for its capability in developing a ratiometric fluorescence probe. To measure GGT activity in ovarian cancer, Shi et al. reported a FRET-mechanism-based ratiometric two-photon fluorescence probe PZS1 (Probe #31) (Figure 18).[78] In this probe, the distance between 7-hydroxycoumarin and the BODIPY chromophore was estimated to be 8.19 Å with a FRET efficiency of 88.8%. Upon GGT-catalyzed cleavage of γ-glutamyl to form PPZS1, the distance was increased to 11.84 Å, resulting in low FRET efficiency. Therefore, the emission of BODIPY at 610 nm was decreased and coumarin's emission at 461 nm increased for a ratiometic fluorescence ($I_{461/610}$) measurement of GGT. The PZS1 is able to undergo two-photon excitation at 700 nm, allowing for two-photon ratiometric fluorescence imaging of GGT activity in ovarian cancer cells.

2.5. Measuring GGT by a Responsive Fluorescence Nanoprobe

Responsive nanoprobe technology has emerged for the biosensing and imaging application for measuring various biomolecules in recent years.[79] In comparison with small molecular probes, cutting edge nanotechnology facilitates huge numbers of luminophores to be loaded into one nanoparticle, thus allowing the prepared nanoprobe for specific biomolecule measurement with higher sensitivity. Moreover, the surface of the nanoparticles could be easily adjusted for biosensing and imaging applications by sophisticated surface modification approaches.[79,80] For example, the surface coating with biocompatible materials or surface conjugation of targeting ligands would allow nanoprobes with minimal cytotoxicity for biomolecules' measurement at specific diseased tissues. Until now, only four nanoprobes have been developed for fluorescence measurement of GGT activity that are discussed in this section.

In 2019, Liu and colleagues described the preparation of a nanoprobe (Probe #32) for GGT fluorescence measurement in living cells and the application in precision medicine (Figure 19).[81] This probe was designed based on exploring the AIE and ESIPT mechanism; i.e., the fluorescence "off−on" response that is essential for GGT measurement could be achieved through a three-step process, including: (i) the GGT-catalyzed cleavage of γ-glutamyl linker on small molecular probe ABTT-Glu and the formation of ABTT product; (ii) the molecular form of ABTT has low water solubility and could aggregate in aqueous solution to form the nanoparticle; and (iii) the aggregation of ABTT switched on the emission due to the AIE triggered ESIPT effect, which is not possible for ABTT and ABTT-Glu as the molecules in solution. This probe

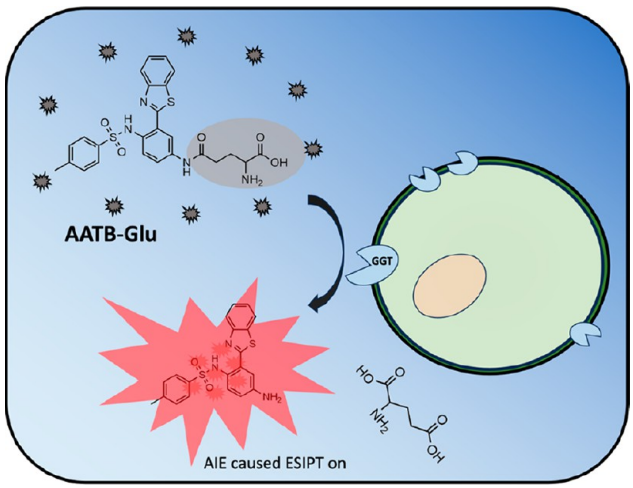

Figure 19. Chemical structure of responsive fluorescence probe ABTT-Glu (Probe #32) and mechanism for this probe in responding to GGT.[81]

showed a fast response (within 30 min) to GGT in the range of 0−90 U/L with LOD 2.9 U/L. Imaging GGT's activity in living HepG2 cells and human liver tissues was then demonstrated using ABTT-Glu as the probe.

Carbon dots (CDs) have emerged as one type of key luminescence nanoparticles for the development of nanoprobes for biosensing and imaging.[82] In designing the CD-based nanoprobe for GGT, the inner filter effect (IFE) has been wildly adopted to quench the emission from CDs. For example, Tong et al. prepared the nitrogen doped CDs (N-CDs) and used the N-CDs (Probe #33) as the nanoprobe for fluorescent GGT measurement.[83] The N-CDs were mixed with γ-L-glutamyl-4-nitroanilide (γ-G4NA); the prepared nanoprobe solution showed intense emission at 510 nm upon excitation at 408 nm. In the presence of GGT, the cleavage of the γ-glutamyl linker from γ-G4NA yielded 4-NA. The overlapping of 4-NA's absorption and N-CDs' excitation promoted the IFE process, thus leading to the quenching of N-CDs' emission. In addition to the "off−on" fluorescence response, the color of the solution changed from colorless to pale yellow, allowing colorimetric measurement of GGT. Then, this nanoprobe was used for GGT measurement in human sera and evaluating GGT inhibitors from extracts of *Schisandra chinensis*.

Cui et al. prepared the biomass quantum dots (BQDs) from cauliflower raw materials and used the BQDs as the nanoprobe (Probe #34) for fluorescent GGT measurement (Figure 20).[84] The cauliflower extract was solvothermally treated, and the formed BQDs were mixed with γ-L-glutamyl-*p*-nitroanilide (GPNA) to measure GGT. The resulting solution showed intense NIR emission at 678 nm upon excitation at 408 nm. The GGT-triggered cleavage of γ-glutamyl linker of GPNA formed P-NA that could quench the NIR emission through the IFE process, similar to the above N-CD nanoprobe.[83] The "on−off" response of the BQDs allowed GGT measurement in the range 0−10 U/L, with an LOD of 0.276 U/L. The applications of the BQDs for GGT imaging in HepG2 cells and GGT's inhibition measurements were then demonstrated. In another study, Tong et al. reported the preparation of dual emission CDs (Probe #35) for fluorescence measurement of GGT and alkaline phosphatase (ALP) activity simultaneously.[85] The CDs prepared from *A. chinensis* showed dual emission at 471 (λ_{ex} = 410 nm) and 671 nm (λ_{ex} = 615 nm). A

https://doi.org/10.1021/acsmeasuresciau.3c00045
ACS Meas. Sci. Au 2024, 4, 54−75

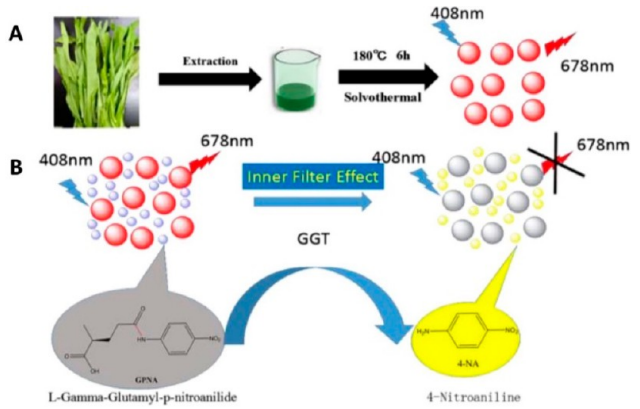

Figure 20. Design of fluorescent BQDs as the probe (Probe #34) for GGT. (A) The procedure for preparing BQDs. (B) Mechanism for mixture of BQDs and GPNA in response with GGT via IFE. Reprinted with permission from ref 84. Copyright 2021 Elsevier.

mixture of CDs with γ-GPNA was then prepared for GGT measurements because the γ-GPNA could respond to GGT to produce P-NA. The P-NA would then quench the blue emission at 471 nm through the IFE process, facilitating the GGT activity measurement with LOD 0.71 U/L.

2.6. Measuring GGT by Other Techniques

Measuring the activity of GGT has also been achieved by alternative techniques, including bioluminescence,[86] chemiluminescence,[87] photoacoustic imaging (PAI),[88] Raman,[89,90] ionizing-radiation-based techniques, like positron emission tomography (PET),[91−93] and magnetic resonance imaging (MRI).[94,95] In comparison with the responsive probes used for fluorescence measurements, the availability of probes employing these techniques for GGT measurements is limited. In this section, advances in the development of probes using these alternative techniques are summarized.

Bioluminescence is the luciferase-catalyzed light emission through the oxidation of some small-molecule-based substrates, like luciferins.[96] As the external light excitation is not required, bioluminescence probes for luminescence measurements are featured with "zero" background noise signal,[97] allowing for highly sensitive biosensing and imaging. Generally, bioluminescence probes using luciferin substrate are designed by modifying the hydroxyl or -NH_2 with analyte-responsive linker.[98] For the GGT-responsive bioluminescence probe (Probe #36) developed by Lin et al. (Figure 21),[86] the -NH_2 of aminoluciferin was caged with γ-glutamyl, which blocked the luciferase catalysis for bioluminescence. Upon cleavage of the γ-glutamyl, aminoluciferin was released, followed by the reaction with luciferase for an "off−on" bioluminescence response for GGT measurement. The bioluminescence at 520 nm was 309-fold enhanced in the presence of 100 U/L GGT, and the LOD was 3.22 U/L for GGT measurement. Using this probe #34 for bioluminescence imaging of GGT expressed by ES-2-luc cells and tumor-bearing mice was then achieved.

Similar to bioluminescence, chemiluminescence that emits from electron-transfer-based chemical reactions is also free from external light excitation, enabling a high S/N ratio for background free luminescence measurements.[99] The development of chemiluminescence probes for biosensing and imaging has received increasing attention in recent years, and a huge number of responsive chemiluminescence probes have been developed,[100] including the probe for GGT activity measurement. For instance, in 2019, An and colleagues reported a chemiluminescence probe (Probe #37) for GGT activity measurement in vitro and in vivo (Figure 22).[87] This probe was developed by incorporating γ-glutamyl with electron-withdrawing acrylic group substituted Schaap's phenoxydioxetane through a *p*-aminobenzyl alcohol self-immolative linker. As for the caged hydroxyl of luminophore, Probe #37 showed inactive chemiluminescence, while when it was switched on after GGT catalysis it initialized cleavages of γ-glutamyl and *p*-aminobenzyl alcohol linker. The chemiluminescence at about 540 nm was 876-fold enhanced for sensitive (LOD 16 mU/L) measurement of GGT. The background free chemiluminescence allowed the probe for measuring GGT activity in serum from lipopolysaccharide (LPS)-treated mouse. Moreover, real-time chemiluminescence imaging of GGT activity in cancer and normal cells and U87MG-tumor-bearing mice were obtained to demonstrate the practical applications of this probe.

As an emerging molecular bioimaging technique, PAI has been able to track the biomolecules in situ in deep tissue with high spatial resolution and S/N ratio.[101] Different from

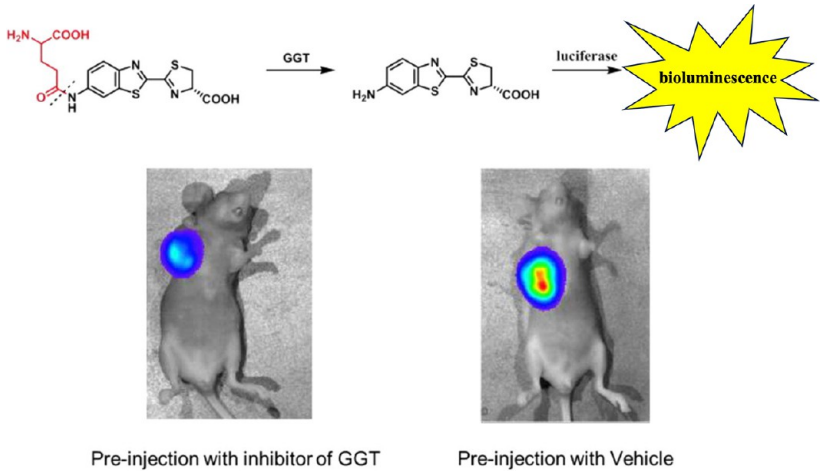

Figure 21. Mechanism of the bioluminescent probe (Probe #36) for GGT measurement and the bioluminescence imaging results of mice with and without GGT inhibitor after injection of the probe. Reprinted with permission from ref 86. Copyright 2018 Elsevier.

https://doi.org/10.1021/acsmeasuresciau.3c00045
ACS Meas. Sci. Au 2024, 4, 54−75

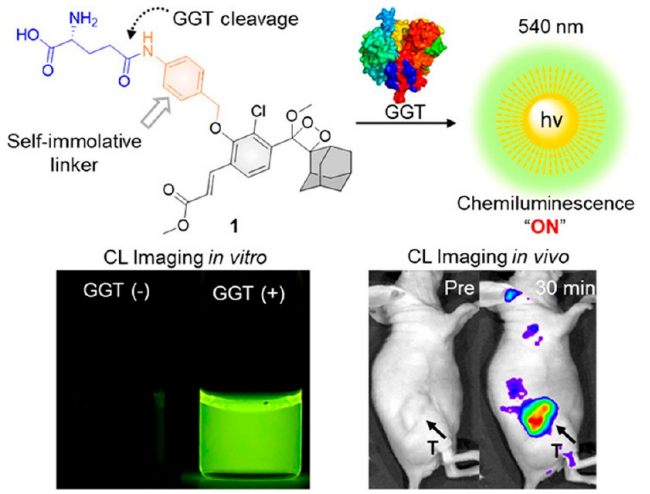

Figure 22. Reaction of the chemiluminescent probe (probe #37) with GGT, change of chemiluminescence in the absence and presence of GGT, and use of this probe for GGT imaging. Reprinted with permission from ref 87. Copyright 2019 American Chemical Society.

fluorescence measurement, excitation to PA endogenous chromophores and exogenous contrast agents leads to the temperature and pressure rise and subsequently the acoustic wave for PA image construction.[102] Despite the high spatial resolution of PAI in in vivo imaging, it is challenging to investigate the biomolecule's variation at (sub)cellular level with the technique.[102] Complementary with fluorescence measurements, a fluorescence-PA bimodal imaging probe (IP, Probe #38) for GGT activity was reported by Miao and colleagues (Figure 23).[88] The IP was developed by coupling GGT-responsive γ-glutamyl to thioxanthene-hemicyanine, the NIR fluorophore, and PA contrast agent. An integrin-targeted peptide (cRGD) was also linked to thioxanthene-hemicyanine through a click reaction for targeting of the liver fibrosis region. Upon the GGT-catalyzed cleavage of γ-glutamyl, a new absorption peak at 730 nm emerged, allowing for conversion of light excitation to acoustic wave for PAI. The fluorescence emission at 770 nm also showed a 36-fold increase, allowing for highly sensitive fluorescence measurement of GGT's activity (LOD = 0.6 mU/L). The cRGD peptide facilitated the IP's accumulation at the liver fibrosis region for targeted fluorescence and PA imaging of GGT's activity in LO2 cells and liver fibrosis in living mice.

As a Raman spectroscopic analysis technique, surface-enhanced Raman spectroscopy (SERS) provides structural fingerprinting of analytes at low concentration with ultrahigh sensitivity and selectivity.[103,104] Therefore, SERS have been widely adopted in various research fields in surface and bio-nanointerface chemistry, biological and biomedical investigations, food and agriculture studies, environmental analyses, etc.[105] In 2020, Jiang et al. reported a SERS probe (Probe #39) for measuring GGT's activity in serum and for investigating GGT's inhibitors.[89] The compound bis-*s*,*s*′((*s*)-4,4′-thiolphenylamide-Glu) (b-(*s*)-TPA-Glu) is able to respond to GGT by cleaving the γ-glutamyl to yield 4,40-disulfanediyldianiline. The disulfide (−S−S−) bond can bind to the surface of silver nanoparticles (AgNPs) to enhance the Raman signal. As a result of the GGT-catalyzed cleavage reaction, a new peak

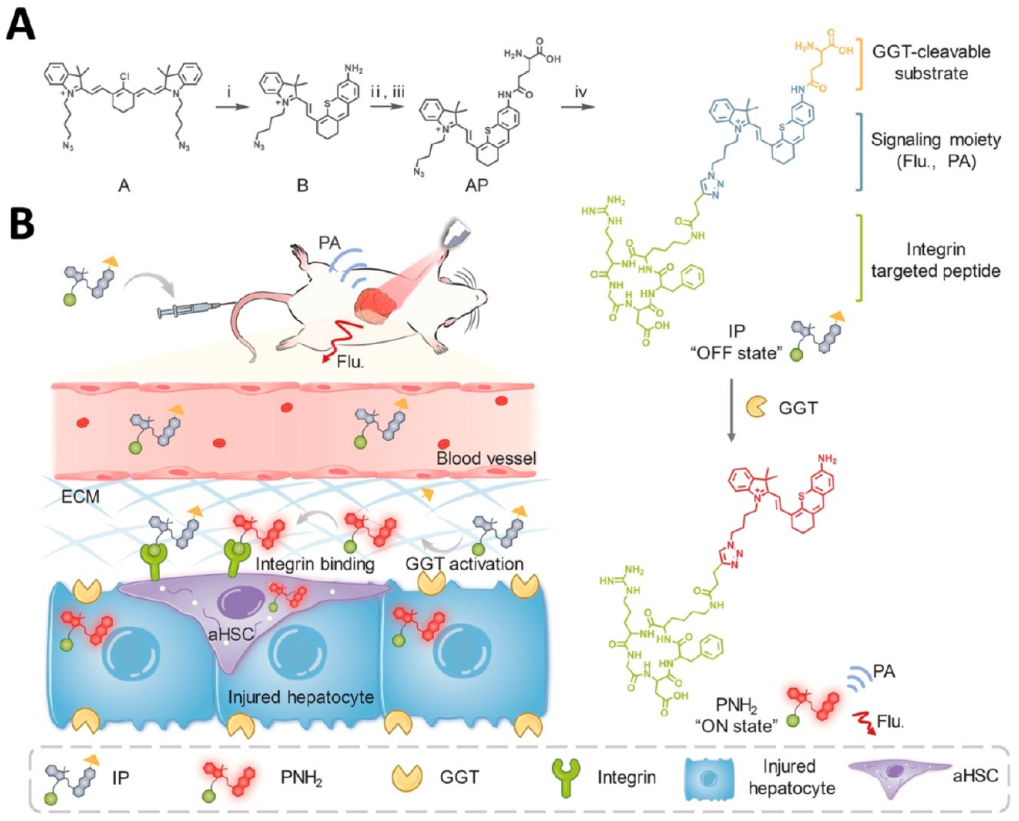

Figure 23. (A) Schematic illustration of the chemical structure and synthesis of the photoacoustic (PA) and fluorescence probe (IP, Probe #38) for integrin-targeted GGT measurement. (B) Schematic representation of IP for NIR fluorescence and PA imaging of liver fibrosis. Reprinted with permission from ref 88. Copyright 2023 Elsevier.

https://doi.org/10.1021/acsmeasuresciau.3c00045
ACS Meas. Sci. Au 2024, 4, 54−75

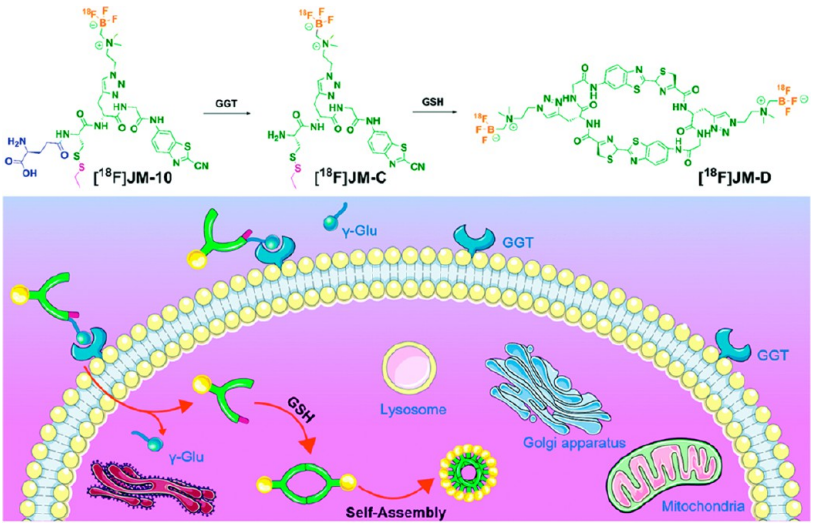

Figure 24. Sensing mechanism of [^{18}F]JM-10 (Probe #42) for GGT measurement. Reprinted with permission from ref 93. Copyright 2022 The Royal Society of Chemistry.

located at 387 cm^{-1} that could be attributed to the C−C−C rocking of the benzene ring and the scissoring of CeCeNH$_2$ emerged. Using the peak at 1075 cm^{-1} (stretching of the benzene ring and scissoring of the C−H bond) as the reference, a ratiometric (I_{387}/I_{1075}) measurement of GGT's activity was achieved. Zhang et al. in another study reported a fluorescence and Raman probe (Probe #40) for GGT activity measurement.[90] The hydroxyl group hemicyanine fluorophore was caged by a cyano group functionalized GSH derivative that could respond to GGT through a cleavage reaction. Uncaging of the fluorophore was then achieved after a spontaneous intramolecular cyclization, and the emission of the fluorophore (λ_{em} = 710 nm) on the surface of gold nanorods (AuNRs)-mesoporous silica was further increased through a plasmon enhanced fluorescence (PEF) mechanism. The release of cyano group compounds resulted in the emergence of a SERS signal at 2250 cm^{-1}. The LOD for GGT measurement was 1.2 and 95 mU/L for the fluorescence and Raman method, respectively.

Considering the fact of GGT overexpression in tumors, radiolabeling by radiocomplex has been reported for cancer diagnosis. For example, Sidiq et al. reported the design of radiocomplex [^{99m}Tc]Tc-GSH and evaluated its performance in labeling of colon cancer.[92] In another study, Ye et al. reported a GGT-activatable fluorine-18 labeled probe (Probe #41) for enhanced PET imaging of tumors.[91] In this study, a fluorine-18 labeled small-molecule probe, [^{18}F]γ-Glu-Cys-(StBu)-PPG(CBT)-AmBF$_3$ (^{18}F-1G), was synthesized. Upon GGT-catalyzed cleavage of γ-glutamyl, intramolecular condensation of the product allowed the formation of a dimer (^{18}F-1-Dimer) that was then self-assembled to form the nanoparticle (^{18}F-1-NPs). The ^{18}F-1G was able to target cancer cells because of the GGT overexpression, which was then confirmed by the PET imaging of HCT116 tumor bearing mice. The [^{18}F]-based PET probe ([^{18}F]JM-10, Probe #42) was also developed by Wang et al. in 2022 for GGT measurement (Figure 24).[93] Interestingly, the probe [^{18}F]JM-10 could respond to GGT on the cell membrane to produce [^{18}F]JM-C. After internalization of [^{18}F]JM-C, [^{18}F]JM-D could be produced that could then be self-assembled through p-stacking to form the nanoparticle with 179 ± 20 nm diameter. The probe [^{18}F]JM-10 was finally applied to measure GGT activity in tumors.

Despite some progress of radiolabeling and PET imaging of GGT activity in vitro and in vivo, the use of these nuclear imaging techniques may lead to toxic side-effects.[106] An alternative technique would be MRI by contrast agents, such as the most commonly used responsive gadolinium (Gd) complexes.[107] For example, Hai and colleagues described the synthesis of a GGT-responsive Gd complex (Glu-Cys(StBu)-Lys(DOTA-Gd)-CBT, 1-Gd) as the probe (Probe #43) for imaging of tumor (Figure 25).[95] In this system, the GGT could cleave the γ-glutamyl to form 1-cleaved that then could be condensed to a 1-Dimer, similar to that of ^{18}F-1G.[91] Self-

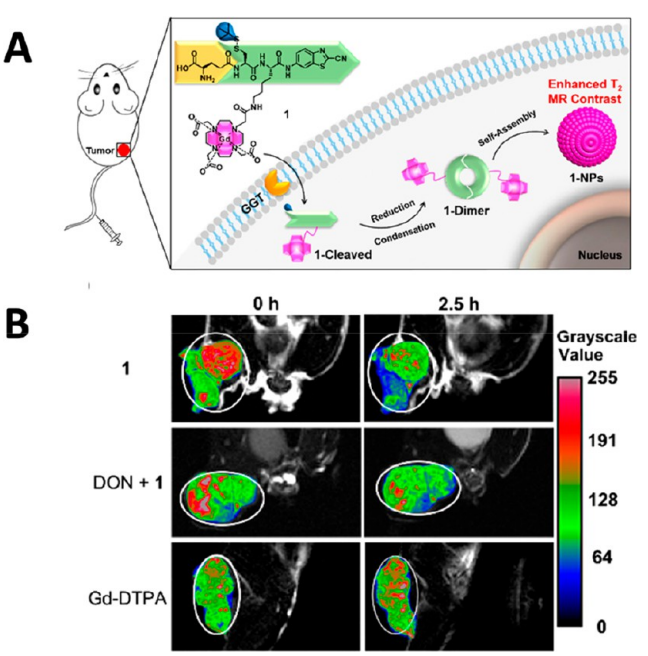

Figure 25. (A) Sensing mechanism for the GGT-responsive Gd complex. (B) T2-weighted coronal MR images of HeLa-tumor-bearing mice injected with DON and Gd-DTPA at different times (0 and 2.5 h). Reprinted with permission from ref 95. Copyright 2019 American Chemical Society.

https://doi.org/10.1021/acsmeasuresciau.3c00045
ACS Meas. Sci. Au 2024, 4, 54−75

assembly of 1-Dimer allowed the formation of nanoparticles (1-NPs), promoting the T_2-weighted MR signal for GGT measurement. In addition to ^{1}H MRI, ^{13}C NMR spectra have also been used for GGT measurement by Nishihara and colleagues.[94] In this case, the ^{13}C-labeled small molecule γ-Glu-[1-^{13}C]Gly that responds to GGT through a cleavage reaction was synthesized. A chemical shift (Δ = 4.3 ppm) from 177.2 to 172.9 ppm was observed after the cleavage, while this shift was not obtained in the presence of a GGT inhibitor, like acivicin.

3. APPLICATIONS OF GGT-ACTIVATABLE FLUORESCENCE MATERIALS

3.1. GGT-Activatable Materials for Cancer Diagnosis

Beyond the measurement of the GGT's activity, GGT-activatable materials have also emerged as a new research topic in biological investigation. Of the different applications, the use of the GGT-activatable materials for cancer diagnosis and treatment, bacterial detection, and inhibitor analysis has been particularly interesting.[32] Cancer remains the predominant cause of mortality across the globe, responsible for approximately one in every six deaths. Timely detection and successful management of cancer within the body are pivotal factors in combating this disease.[50] Previous studies have clearly identified the elevated GGT levels in cancer, e.g., 494.5765 U/L of GGT in HeLa cells,[73] while 5−85 U/L in blood of normal adult.[39] Taking this fact into consideration, GGT has been explored as a potential diagnostic and prognostic biomarker for various cancers.[108]

As introduced above, Urano and co-workers developed an "off−on" response fluorescence probe (γGlu-HMRG, Probe #1) for GGT measurement. The GGT could cleave the γ-glutamyl from γGlu-HMRG to release the fluorescent HMRG that was then rapidly internalized into cells and accumulated primarily in lysosomes to promote the fluorescence specifically in enzyme-expressing cells (Figure 2).[23] Spraying of γGlu-HMRG to the tumor tissue lit up the fluorescence signals within 1 min. For other normal tissues, fluorescence signal was not observed due to the limited expression of GGT, which created a high signal-to-noise (S/N) ratio for cancer diagnosis. Following research included spraying γGlu-HMRG for rapid diagnosis of metastatic lymph nodes (mLNs) of colorectal cancer,[109] for visualization of the leakage of pancreatic juice after digestive surgery,[110] and for colorectal tumor imaging,[111] intravenous administration of γGlu-HMRG for deeply located tumors, like lung tumor diagnosis,[112,113] and urinalysis of GGT for diagnosis of diabetic kidney and glomerular diseases.[114]

3.2. GGT-Activatable Materials for Bacterial Measurement and Isolation

Elevated expression of GGT has also been revealed in *Helicobacter pylori* infections.[115] Using γGlu-HMRG as the probe, Akashi et al. then evaluated the *Helicobacter pylori* infection by recording the changes of fluorescence signals at 5 and 15 min post initial exposure to γGlu-HMRG.[116] The sensitivity and specificity were 75.0% and 83.3% in the antrum and 82.6% and 89.5% in the stomach body, suggesting the potential of this probe for rapid diagnosis of *Helicobacter pylori* infections. In addition to the *Helicobacter pylori* infection, bacterial proliferation also produces high levels of GGT. In another study by Wang and co-workers, glutamic acid was conjugated to 7-amino-1,3-dichloro-9,9-dimethylacridin-2(9*H*)-one (DDAN) fluorophore to fabricate DDAG (Probe #44) for NIR fluorescence analysis of bacterial GGT and screening of GGT inhibitors (Figure 26).[117] The cleavage of the γ-glutamyl linker led to the formation of DDAN with the

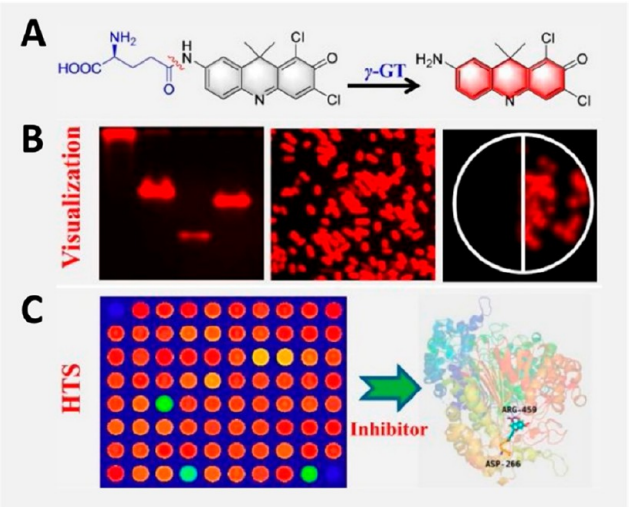

Figure 26. (A) Chemical structure of DDAG (Probe #44) and sensing mechanism of this probe for GGT measurement. (B) The native PAGE-gel electrophoresis for different bacterial lysates stained with DDAG and fluorescence imaging for bacteria in liquid culture and agar plate. (C) The fluorescence imaging for discovery of GGT inhibitors and in silico docking analysis for them. Reprinted with permission from ref 117. Copyright 2021 Elsevier.

sensing mechanism similar to other GGT fluorescence probes. Red shifts of the absorption spectra and the enhancement of fluorescence at 667 nm were observed after the cleavage reaction. Different from other responsive probes, the DDAG showed its capability in measuring GGT activity in various bacteria including *Pseudomonas aeruginosa*, *Escherichia coli*, *Enterobacter aerogenes*, *Bacillus cereus*, *Acinetobacter baumannii*, and *Enterococcus faecalis*. Investigation of inhibitors from natural compounds and herbal medicines was then conducted to identify the baicalein, myricetin, and amaronol A from herbal medicines for GGT inhibition.

Isolation of GGT rich bacteria from mouse gut has also been achieved using a "off−on" response fluorescence probe (ADMG, Probe #45) developed by Liu and colleagues.[118] The emission at 670 nm (λ_{ex} = 456 nm) was enhanced after the GGT-catalyzed cleavage of the γ-glutamyl linker. Fluorescence in vivo imaging of intestinal bacteria revealed high bacterial GGT level at the duodenum section. The GGT levels could be decreased when applying antibiotics, such as ampicillin, metronidazole, neomycin, and vancomycin. Dissection of mice guts allowed the collection of intestinal bacteria, which were then identified to be *K. pneumoniae CAV1042*, *K. pneumoniae XJRML-1*, and *E. faecalis* using 16sDNA analysis.

Another interesting application of the GGT-activation involves nucleolus targeting specifically for cancer cells. In 2022, Xue and co-workers grafted glutamic acid to indole-quinolinium (QI) through an L-proline-glycine dipeptide linker.[119] The formed QI-PG-Glu (Probe #46) is able to be activated by GGT through a two-step process, including (i) GGT-catalyzed cleavage of γ-glutamyl and (ii) rapid self-driven cyclization of the L-proline-glycine dipeptide linker. Release of HQI dye is not fluorescent, while it can specifically bind to the nucleolus to switch on emission at 578 nm. This GGT-

https://doi.org/10.1021/acsmeasuresciau.3c00045
ACS Meas. Sci. Au 2024, 4, 54−75

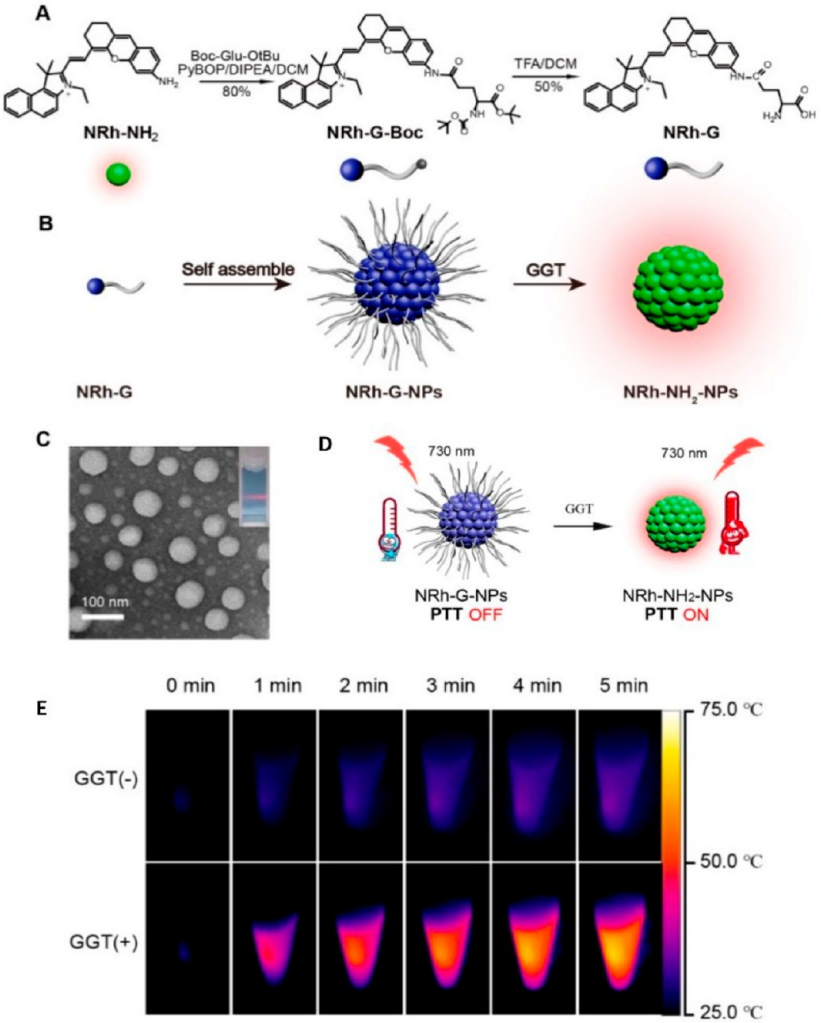

Figure 27. (A) Chemical structure and synthesis procedure of NRh-G. (B) Processes of NRh-G capsuled into nanoparticles and reacting with GGT. (C) TEM image of NRh-G-NPs. (D) Schematic diagram of the photothermal property turning on. (E) Infrared thermography was performed on NPs under varying temperature and time gradients, both in the presence and absence of GGT. Reprinted with permission under a Creative Commons Attribution 4.0 International License from ref 128. Copyright 2021 Ivyspring International Publisher.

activated HQI showed capabilities in restricting RNA Polymerase I transcription, resulting in cell apoptosis. Together with the fact of high expression of GGT in cancer cells, this GGT-activatable material has the potential for cancer diagnosis and treatment.

3.3. GGT-Activatable Materials for Cancer Therapy

Precision medicine for cancer treatment plays a pivotal role in improving the therapeutic efficacy for cancer patients.[50] Currently, most of the medicines, including the targetable nanomedicine, exhibit limited treatment efficiency because of the high risk of side effects. To address this issue, customized medicines would be more suitable because the anticancer drugs can only be activated at the specific tumor tissues by responding to the tumor microenvironment (TME), such as acidic condition, hypoxia, and high redox levels.[50] For example, phototherapy, including photodynamic therapy (PDT) and photothermal therapy (PTT), has been particularly interesting over other treatment procedures because the use of toxic anticancer drugs is not required,[120] minimizing the side effects.[45] However, phototherapy necessitates that patients remain in a dark room both during the treatment process and in the subsequent days.[121] This precaution is necessary because the photosensitizers generate a substantial quantity of reactive oxygen species (ROS) for PDT and heat for PTT upon exposure to natural light.[120] Caging the photosensitizers by chemical modification would be able to tackle this problem, in which the modified photosensitizers are photoinactive while activation in TME allows photosensitizers for production of ROS and heat for cancer treatment.

Realizing that the γ-glutamyl linker could be specifically cleaved by GGT in tumor tissue,[23] Chiba et al. reported the development of an activatable photosensitizer (γGlu-HMSeR) for PDT through caging hydroxymethyl selenorhodamine green photosensitizer (HMDESeR) with a GGT-activatable γ-glutamyl linker.[122] The γGlu-HMSeR is photoinactive, while, in the presence of GGT in TME, the HMDESeR would be released. The HMDESeR photosensitizer showed a high singlet oxygen ($^1O_2$) quantum yield (Φ_Δ = 0.74, similar to Rose Bengal Φ_Δ = 0.75 in PBS of pH 7.4) to kill the cancer cells and tumor in a chick chorioallantoic membrane model. Similarly, an asymmetric bismuth-rhodamine (BiRGlu) has also been developed by Mukaimine et al. as the GGT-activatable photosensitizer for PDT.[123] In similar research, Yang et al. modified the chemical structure of diketopyrrolo-

https://doi.org/10.1021/acsmeasuresciau.3c00045
ACS Meas. Sci. Au 2024, 4, 54−75

Table 1. Summary of the Responsive Probes for GGT Measurement[a]

Number	$\lambda_{ex}/\lambda_{em}$ (nm)	Limit of Detection	Linearity Range	Condition	Ref.
1	501/524	-	0−80 U/L	PBS, pH 7.4, 1% DMSO	23
2	460/530	0.029 U/L	0−10 U/L	0.1 M sodium phosphate buffer, pH 7.4, 0.1% DMSO	33
3	580/632	0.5 U/L	5−100 U/L	10 mM PBS, pH 7.4, 1% DMSO	34
4	585/615	5.6 mU/L	1−50 U/L	PBS, pH 7.4	35
5	470/578	0.0702 U/L	0−30 U/L	PBS, pH 7.4	36
6	360/472	0.59 U/L	0−10 U/L	10 mM PBS, pH 7.4, 37 °C	39
7	370/500	16.7 mU/L	0.05−80 U/L	10 mM PBS, pH 7.4, 0.1% DMSO	40
8	520/605	41 mU/L	0−50 U/L	PBS, pH 7.4	41
9	362/473	210 mU/L	0−22 U/L	PBS, pH 7.4, 25 °C	42
10	730/780	7.6 mU/L	0−100 U/L	10 mM HEPES, pH 7.4, 37 °C	47
11	680/708	0.5 U/L	1−75 U/L	PBS, pH 7.4	49
12	680/720	3.6 mU/L	0.2−5 U/L	PBS, pH 7.4	51
13	660/712	2.91 mU/L	0.02−5 U/L	PBS, pH 7.4	52
14	687/714	-	0−0.05 U/mL	PBS, pH 7.4	53
15	680/710	1.2 U/L	5−200 U/L	PBS, pH 7.4	54
16	680/727	0.4 U/L	1−90 U/L	10 mM PBS, pH 7.4, 1.5% DMSO	55
17	640/675	-	0−20 U/L	PBS, pH 7.4	59
18	515/654	51.4 mU/L	0−2 U/mL	PBS, pH 7.4	60
19	445/650	24 mU/L	0−10 mU/L	10 mM PBS, pH 7.4	46
20	490, 820/635	0.057 U/L	0−35 U/L	10 mM PBS, pH 7.4, 37 °C	13
21	330/490	147 mU/L	0.2−5 U/L	PBS with 5% DMSO and 0.2% Triton, pH 7.4	64
22	405, 800/490	0.117 U/L	1−60 U/L	10 mM PBS, pH 7.4, 37 °C	65
23	380/452, 494	0.042 U/L	0−100 U/L	PBS, pH 7.4	69
24	600/670	78.5 mU/L	0−25 U/L	PBS:DMSO = 4:1, v/v; pH 7.4, 37 °C	70
25	398/500, 560	0.23 μM	0−50 U/L	10 mM PBS, pH 7.4, 1% DMSO	71
26	480/580, 625	-	-	PBS, 37 °C	72
27	417, 800/531	182 U/L	230−2200 U/L	PBS, pH 7.4	73
28	470, 850/570	2.27 U/L	0−50 U/L	10 mM PBS, pH 7.4, <1% DMSO	74
29	420, 850/544, 610	1.47 U/L	0−50 U/L	10 mM PBS, pH 7.4, 0.1% BSA, <1% DMSO	75
30	385/456, 527	-	-	10 mM PBS, pH 7.4	77
31	350/461, 610	-	-	0.01 mM PBS, pH 7.4	78
32	365/650	2.9 U/L	0−90 U/L	10 mM PBS, pH 7.4, 37 °C	81
33	408/510	0.6 U/L	2−10 U/L, 10−110 U/L	10 mM PBS, pH 7.4	83
34	408/678	0.276 U/L	0−10 U/L	PBS, pH 7.4, 37 °C	84
35	410, 615/471, 671	0.71 U/L	2.5−90 U/L	10 mM Tris−HCl, pH 8.0, 37 °C	85
36	355/520	3.22 U/L	0−100 U/L	50 mM Tris−HCl, pH 7.4, 10 mM $MgCl_2$	86
37	405/540	16 mL/U	0−250 U/L	PBS, pH 7.4, 37 °C, 5% DMSO	87
38	730/770	6×10^{-4} U/mL	0−0.05 U/mL	10 mM PBS, pH 7.4, 37 °C	88
39	-	0.09 U/L	0.2−200 U/L	PBS, pH 7.4, 37 °C	89
40	-	1.2 mU/L	0−1 U/L	PBS, pH 7.4, 37 °C	90
41	-	-	-	Tris−HCl, pH 8.0, 0.05% Tween@20, 0.4% DMSO, 1 mM DTT	91
42	-	-	-	PBS, pH 7.4	93
43	-	-	-	PBS, pH 7.4, 37 °C	95
44	615/667	-	0−25 μg/mL	PBS, pH 7.4, 37 °C	117
45	456/670	0.036 U/mL	0−1.4 U/mL	KH_2PO_4−K_2HPO_4 buffer, pH 8.0, 37 °C, phosphate buffer−acetonitrile v/v = 2:1	118
46	420/549	-	-	PBS, pH 7.4, 1% DMSO; 0.02% Tween-20	119
47	540/580	-	-	PBS, pH 7.4	125

[a]"-": Not provided in original publication.

pyrrole (DPP)-based photosensitizers (DPP-py) with glutamic acid through a 4-methyl-phenyl linker.[124] The GGT-catalyzed cleavage of γ-glutamyl from DPP-GGT resulted in the formation of the final DPP-py photosensitizer. The red emission (λ_{em} = 672 nm) of DPP-GGT was blue-shifted to yellow (λ_{em} = 548 nm), allowing ratiometric fluorescence measurement and imaging of GGT activity in HepG2 and MCF-7 cancer cells. Upon the light irradiation at 530 nm (20 mW/cm^2), the DDP-py produced ROS for cancer cell killing in vitro and HepG2 tumor bearing mouse.

In 2021, Li et al. reported a GGT-activatable small molecule (Glu-RdEB) as the probe for tumor imaging and photosensitizer for PDT.[125] The Glu-RdEB (Probe #47) encompasses three parts, including (i) GGT-cleavage γ-glutamyl

https://doi.org/10.1021/acsmeasuresciau.3c00045
ACS Meas. Sci. Au 2024, 4, 54−75

conjugated self-immolative linker for tumor specific activation; (ii) 5-(ethylamino)-9-diethylaminobenzo-[*a*]-phenothiazinium (ENBS) photosensitizer for ROS production; and (iii) rhodamine (Rd) fluorophore as the signaling unit for fluorescence measurement and imaging. In this Glu-RdEB structure, the emission of Rd was quenched by ENBS that is photoinactive in the absence of GGT. Upon GGT-catalyzed hydrolysis, fluorescent Rd and ENBS were released for fluorescence imaging and $^1O_2$ production upon light irradiation (660 nm, 300 mW/cm^2). This GGT-activatable photosensitizer was then used for U87 cancer cell killing and tumor growth inhibition in a mouse model.

In addition to PDT, PTT in which the local temperature increases upon light irradiation, has also been widely adopted for cancer therapy.[126,127] For instance, Zhou et al. prepared a GGT-activatable nanoparticle for NIR fluorescence imaging guided PTT in 2021 (Figure 27).[128] Conjugating the glutamic acid with cyanine dye (NRh-NH$_2$) through a γ-glutamyl linker, the formed NRh-G would be spontaneously assembled into 50−60 nm nanosphere NRh-G-NPs in water. Upon the reaction with GGT, the nonfluorescent NRh-G-NPs showed high fluorescence at 740 nm, which was attributed to the cleavage of γ-glutamyl linker to form fluorescent NRh-NH$_2$-NPs. Moreover, the emergence of a new absorption band at 714 nm allowed NRh-NH$_2$-NPs for converting light to heat for PTT. Upon light irradiation (730 nm, 1.0 W/cm^2 for 5 min), the temperature increased from 36 to 54 °C in U87MG tumor-bearing mice after the intravenous injection of NRh-G-NPs, demonstrating the capability of NRh-G-NPs for cancer PTT.

4. CONCLUDING REMARKS

This review summarizes the advances in the development of responsive probes for measuring GGT's activity both in vitro and in vivo and highlights the practical applications of GGT-activatable materials. Regarding the responsive probes for fluorescence measurement of GGT activity, advances in the development of "off−on", ratiometric, two-photon, and NIR fluorescence probes were overviewed. Alternative probe technology, such as the probes based on bioluminescence, chemiluminescence, MRI, PET, PA, and SERS, was then summarized. The performance of the responsive probe for GGT measurement was summarized in Table 1.

In comparison with responsive probes for the fluorescence measurement of GGT, limited numbers of alternative probes are currently available, which might be attributed to the unique advantages of fluorescence bioassay in vitro and in vivo. The practical applications of the GGT-activatable materials for cancer diagnosis and therapy (e.g., PDT and PTT), bacterial determination, and purification were also highlighted. Through systematic analysis of the publications, we determined the unique strengths and inherent limitations of each responsive probe and activatable materials and proposed the following research in the field:

(1) In terms of the responsive probe technology in bioassay, a number of probes have been successfully developed as tools for measuring GGT activity by recording the signals of fluorescence, bioluminescence, chemiluminescence, MRI, PET, Raman, and PA. It is clear that the responsive probes for fluorescence analysis have been widely investigated due to their unique advantages, such as high sensitivity and selectivity, low cost, simplicity, and high resolution in bioimaging. The limitations of this method, such as poor tissue penetration of the light excitation and emission, light scattering, and autofluorescence from biological systems, should be considered in further developing of responsive fluorescence probes for GGT. Interestingly, recent studies have demonstrated the bi- (or multi-) modal probes, such as fluorescence-PA[88] and fluorescence-Raman[90] probes for precise and accurate measurement of GGT activity in vitro and in vivo. Therefore, the development of bi- (or multi-) modal probes would be more preferable in future studies.

(2) For the development of almost all responsive probes, the GGT-catalyzed cleavage of γ-glutamyl linker is the sensing mechanism, and this cleavage reaction generally takes a few minutes to hours. For fast measurement of GGT activity, the discovery of an innovative sensing mechanism for the development of new responsive probes is highly demanded.

(3) GGT has been identified as the cell-membrane-bound enzyme that contributes to maintaining cellular homeostasis of GSH and derivatives. Although a few responsive probes have been developed for intracellular GGT measurement, these probes could respond to GGT at the cell membrane and then the sensing reaction products could be internalized into the cells. To address this issue, a few probes (e.g., GGTIN-1[53] and mNVPy_Glu[75]) have been developed for GGT measurement on cell membranes. These probes are promising for precise and accurate measurement of GGT activity in situ, in vitro, and in vivo.

(4) Regarding the GGT-activable materials for practical applications, the GGT-activated phototherapy (PDT and PDT) is particularly interesting. In this type of phototherapy, the caged photosensitizers are insensitive to light, while the GGT-activated photosensitizers in situ could be used for killing cancer cells and bacteria, allowing for high treatment efficiency with minimal side effects. Therefore, the development of GGT-activatable photosensitizers and medicines would be one of the directions in future studies.

In conclusion, we believe that this comprehensive review will contribute to guiding future research on the development of responsive probes for GGT activity analysis and the fabrication of new GGT-activatable materials. Given the rapid progress of the research field, we are convinced that the new generation of GGT responsive probes and activatable materials would be developed for (pre)clinical applications in diseases' early diagnostic, treatment, and treatment monitoring in the not-too-distance future.

AUTHOR INFORMATION

Corresponding Author

Run Zhang − *Australian Institute for Bioengineering and Nanotechnology, The University of Queensland, St. Lucia, Queensland 4072, Australia;* orcid.org/0000-0002-0943-824X; Email: r.zhang@uq.edu.au

Authors

Yiming Zhang − *Australian Institute for Bioengineering and Nanotechnology, The University of Queensland, St. Lucia, Queensland 4072, Australia*

https://doi.org/10.1021/acsmeasuresciau.3c00045
ACS Meas. Sci. Au 2024, 4, 54−75

Zexi Zhang − *Australian Institute for Bioengineering and Nanotechnology, The University of Queensland, St. Lucia, Queensland 4072, Australia;* orcid.org/0000-0001-7805-5448

Miaomiao Wu − *Australian Institute for Bioengineering and Nanotechnology, The University of Queensland, St. Lucia, Queensland 4072, Australia;* orcid.org/0000-0002-6572-6721

Complete contact information is available at: https://pubs.acs.org/10.1021/acsmeasuresciau.3c00045

Author Contributions

The manuscript was written through the contributions of all authors. All authors have approved the final version of the manuscript. CRediT: **Yiming Zhang** writing-original draft; **Zexi Zhang** writing-review & editing; **Miaomiao Wu** writing-review & editing; **Run Zhang** conceptualization, funding acquisition, project administration, supervision, writing-original draft, writing-review & editing.

Notes

The authors declare no competing financial interest.

■ ACKNOWLEDGMENTS

The authors gratefully acknowledge the financial support from the National Health and Medical Research Council (APP1175808). Z.Z. wishes to acknowledge the UQ Entrepreneurial PhD Top-Up Scholarship and Andrew N. Liveris Academy. Assistance of the Australian Microscopy & Microanalysis Research Facility at the Centre for Microscopy and Microanalysis (CMM) and Queensland Node of the Australian National Fabrication Facility (ANFF-Q), the University of Queensland, is also acknowledged.

■ REFERENCES

(1) Singh, H.; Tiwari, K.; Tiwari, R.; Pramanik, S. K.; Das, A. Small Molecule as Fluorescent Probes for Monitoring Intracellular Enzymatic Transformations. *Chem. Rev.* **2019**, *119* (22), 11718−11760.

(2) Liu, H.-W.; Chen, L.; Xu, C.; Li, Z.; Zhang, H.; Zhang, X.-B.; Tan, W. Recent progresses in small-molecule enzymatic fluorescent probes for cancer imaging. *Chem. Soc. Rev.* **2018**, *47* (18), 7140−7180.

(3) Chen, D.; Qin, W.; Fang, H.; Wang, L.; Peng, B.; Li, L.; Huang, W. Recent progress in two-photon small molecule fluorescent probes for enzymes. *Chin. Chem. Lett.* **2019**, *30* (10), 1738−1744.

(4) Chin, J.; Kim, H.-J. Near-infrared fluorescent probes for peptidases. *Coord. Chem. Rev.* **2018**, *354*, 169−181.

(5) Goldberg, D. M. Structural, Functional, and Clinical Aspects of γ-Glutamyltransferase. *CRC Critical Reviews in Clinical Laboratory Sciences* **1980**, *12* (1), 1−58.

(6) Luo, Z.; An, R.; Ye, D. Recent Advances in the Development of Optical Imaging Probes for γ-Glutamyltranspeptidase. *ChemBioChem.* **2019**, *20* (4), 474−487.

(7) Thompson, G. A.; Meister, A. Interrelationships between the binding sites for amino acids, dipeptides, and gamma-glutamyl donors in gamma-glutamyl transpeptidase. *J. Biol. Chem.* **1977**, *252* (19), 6792−6798.

(8) Takemura, K.; Board, P. G.; Koga, F. A Systematic Review of Serum γ-Glutamyltransferase as a Prognostic Biomarker in Patients with Genitourinary Cancer. *Antioxidants* **2021**, *10*, 549.

(9) Corti, A.; Duarte, T. L.; Giommarelli, C.; De Tata, V.; Paolicchi, A.; Jones, G. D. D.; Pompella, A. Membrane gamma-glutamyl transferase activity promotes iron-dependent oxidative DNA damage in melanoma cells. *Mutation Research/Fundamental and Molecular Mechanisms of Mutagenesis* **2009**, *669* (1), 112−121.

(10) Pompella, A.; Corti, A.; Paolicchi, A.; Giommarelli, C.; Zunino, F. γ-Glutamyltransferase, redox regulation and cancer drug resistance. *Current Opinion in Pharmacology* **2007**, *7* (4), 360−366.

(11) Raulf, M.; Stüning, M.; König, W. Metabolism of leukotrienes by L-gamma-glutamyl-transpeptidase and dipeptidase from human polymorphonuclear granulocytes. *Immunology* **1985**, *55* (1), 135−47.

(12) Lee, D.-H.; Gross, M. D.; Steffes, M. W.; Jacobs, D. R. Is Serum Gamma-Glutamyltransferase a Biomarker of Xenobiotics, Which Are Conjugated by Glutathione? *Arterioscler., Thromb., Vasc. Biol.* **2008**, *28* (4), e26−e28.

(13) Zhang, P.; Jiang, X. -f.; Nie, X.; Huang, Y.; Zeng, F.; Xia, X.; Wu, S. A two-photon fluorescent sensor revealing drug-induced liver injury via tracking γ-glutamyltranspeptidase (GGT) level in vivo. *Biomaterials* **2016**, *80*, 46−56.

(14) Kunutsor, S. K. Gamma-glutamyltransferase—friend or foe within? *Liver International* **2016**, *36* (12), 1723−1734.

(15) Suzuki, H.; Fukuyama, K.; Kumagai, H. Bacterial γ-glutamyltranspeptidases, physiological function, structure, catalytic mechanism and application. *Proceedings of the Japan Academy, Series B* **2020**, *96* (9), 440−469.

(16) SILVA, I. S.; FERRAZ, M. L. C.; PEREZ, R. M.; LANZONI, V. P.; FIGUEIREDO, V. M.; SILVA, A. E. Role of γ-glutamyl transferase activity in patients with chronic hepatitis C virus infection. *Journal of Gastroenterology and Hepatology* **2004**, *19* (3), 314−318.

(17) Selinger, M. J.; Matloff, D. S.; Kaplan, M. M. γ-Glutamyl transpeptidase activity in liver disease: serum elevation is independent of hepatic GGTP activity. *Clin. Chim. Acta* **1982**, *125* (3), 283−290.

(18) Smith, G. S.; Walter, G. L.; Walker, R. M. Chapter 18 - Clinical Pathology in Non-Clinical Toxicology Testing. In *Haschek and Rousseaux's Handbook of Toxicologic Pathology*, 3rd ed.; Haschek, W. M., Rousseaux, C. G., Wallig, M. A., Eds.; Academic Press: Boston, MA, 2013; pp 565−594.

(19) Kazemi-Shirazi, L.; Endler, G.; Winkler, S.; Schickbauer, T.; Wagner, O.; Marsik, C. Gamma Glutamyltransferase and Long-Term Survival: Is It Just the Liver? *Clinical Chemistry* **2007**, *53* (5), 940−946.

(20) Turgut, O.; Tandogan, I. Gamma-glutamyltransferase to Determine Cardiovascular Risk: Shifting the Paradigm Forward. *Journal of Atherosclerosis and Thrombosis* **2011**, *18* (3), 177−181.

(21) Jiang, S.; Jiang, D.; Tao, Y. Role of gamma-glutamyltransferase in cardiovascular diseases. *Exp Clin Cardiol* **2013**, *18* (1), 53−6.

(22) Jacobs, W. L. W. γ-Glutamyl-transpeptidase in diseases of the liver, cardiovascular system and diabetes mellitus. *Clin. Chim. Acta* **1972**, *38* (2), 419−434.

(23) Urano, Y.; Sakabe, M.; Kosaka, N.; Ogawa, M.; Mitsunaga, M.; Asanuma, D.; Kamiya, M.; Young, M. R.; Nagano, T.; Choyke, P. L.; Kobayashi, H. Rapid Cancer Detection by Topically Spraying a γ-Glutamyltranspeptidase−Activated Fluorescent Probe. *Science Translational Medicine* **2011**, *3* (110), 110ra119.

(24) Jo, S.-K.; Lee, W.-Y.; Rhee, E.-J.; Won, J.-C.; Jung, C.-H.; Park, C.-Y.; Oh, K.-W.; Park, S.-W.; Kim, S.-W. Serum γ-glutamyl transferase activity predicts future development of metabolic syndrome defined by 2 different criteria. *Clin. Chim. Acta* **2009**, *403* (1), 234−240.

(25) Takahashi, Y.; Soejima, Y.; Fukusato, T. Animal models of nonalcoholic fatty liver disease/nonalcoholic steatohepatitis. *World J. Gastroenterol* **2012**, *18* (19), 2300−8.

(26) Teufel, A.; Itzel, T.; Erhart, W.; Brosch, M.; Wang, X. Y.; Kim, Y. O.; von Schönfels, W.; Herrmann, A.; Brückner, S.; Stickel, F.; Dufour, J.-F.; Chavakis, T.; Hellerbrand, C.; Spang, R.; Maass, T.; Becker, T.; Schreiber, S.; Schafmayer, C.; Schuppan, D.; Hampe, J. Comparison of Gene Expression Patterns Between Mouse Models of Nonalcoholic Fatty Liver Disease and Liver Tissues From Patients. *Gastroenterology* **2016**, *151* (3), 513−525.e0.

(27) Kiuchi, K.; Kiuchi, K.; Nagatsu, T.; Togari, A.; Kumagai, H. Highly sensitive assay for γ-glutamyltranspeptidase activity by high-

performance liquid chromatography with electrochemical detection. *Journal of Chromatography A* **1986**, *357*, 191−198.
(28) Orlowski, M.; Meister, A. γ-Glutamyl-p-nitroanilide: A new convenient substrate for determination and study of l- and d-γ-glutamyltranspeptidase activities. *Biochimica et Biophysica Acta (BBA) - Specialized Section on Enzymological Subjects* **1963**, *73* (4), 679−681.
(29) Kulhánek, V.; Dimov, D. M. A new useful modification for the determination of γ-glutamyltranspeptidase activity. *Clin. Chim. Acta* **1966**, *14* (5), 619−623.
(30) Bruemmer, K. J.; Crossley, S. W. M.; Chang, C. J. Activity-Based Sensing: A Synthetic Methods Approach for Selective Molecular Imaging and Beyond. *Angew. Chem., Int. Ed.* **2020**, *59* (33), 13734−13762.
(31) Han, H.-H.; Tian, H.; Zang, Y.; Sedgwick, A. C.; Li, J.; Sessler, J. L.; He, X.-P.; James, T. D. Small-molecule fluorescence-based probes for interrogating major organ diseases. *Chem. Soc. Rev.* **2021**, *50* (17), 9391−9429.
(32) Saleem, M.; Hanif, M.; Rafiq, M.; Raza, H.; Ja, K. S.; Lu, C. γ-Glutamyltranspeptidase (GGT) Sensitive Fluorescence Probes for Cancer Diagnosis; Brief Review. *J. Fluoresc.* **2023**, DOI: 10.1007/s10895-023-03353-6.
(33) Li, Z.; Li, Y.; Liu, Y.; Zheng, Y.; Shen, J.; He, X.; Peng, B. One-step activated fluorescence bioimaging of γ-glutamyltransferase activity in living cancer cells based on chloro-rhodamine probe. *Dyes Pigm.* **2022**, *199*, 109962.
(34) Wang, K.; Wang, W.; Chen, X.-Y.; Yang, Y.-S.; Zhu, H.-L. Constructing a novel fluorescence detection method for γ-glutamyltranspeptidase and application on visualizing liver injury. *Biosens. Bioelectron.* **2023**, *219*, 114767.
(35) Li, L.; Shi, W.; Wang, Z.; Gong, Q.; Ma, H. Sensitive Fluorescence Probe with Long Analytical Wavelengths for γ-Glutamyl Transpeptidase Detection in Human Serum and Living Cells. *Anal. Chem.* **2015**, *87* (16), 8353−8359.
(36) Guo, S.; Zhu, T.; Wang, R.; Gao, J.; Sun, J.; Ou-Yang, Z.; Liu, Y.; Gu, X.; Zhao, C. A water-soluble fluorescent probe for real-time visualization of γ-glutamyl transpeptidase activity in living cells. *Bioorg. Med. Chem. Lett.* **2022**, *68*, 128762.
(37) He, X.; Xiong, L.-H.; Huang, Y.; Zhao, Z.; Wang, Z.; Lam, J. W. Y.; Kwok, R. T. K.; Tang, B. Z. AIE-based energy transfer systems for biosensing, imaging, and therapeutics. *TrAC Trends in Analytical Chemistry* **2020**, *122*, 115743.
(38) Niu, G.; Zhang, R.; Shi, X.; Park, H.; Xie, S.; Kwok, R. T. K.; Lam, J. W. Y.; Tang, B. Z. AIE luminogens as fluorescent bioprobes. *TrAC Trends in Analytical Chemistry* **2020**, *123*, 115769.
(39) Hou, X.; Zeng, F.; Wu, S. A fluorescent assay for γ-glutamyltranspeptidase via aggregation induced emission and its applications in real samples. *Biosens. Bioelectron.* **2016**, *85*, 317−323.
(40) Ou-Yang, J.; Li, Y.-F.; Wu, P.; Jiang, W.-L.; Liu, H.-W.; Li, C.-Y. Detecting and Imaging of γ-Glutamytranspeptidase Activity in Serum, Live Cells, and Pathological Tissues with a High Signal-Stability Probe by Releasing a Precipitating Fluorochrome. *ACS Sensors* **2018**, *3* (7), 1354−1361.
(41) Xie, H.; Gao, J.; Sun, X.; Song, Y.; Zhang, Q.; Zhang, P.; Ding, C. A water-soluble fluorescent probe for the determination of γ-glutamyltransferase activity and its application in tumor imaging. *Talanta* **2023**, *253*, 123943.
(42) Tong, H.; Zheng, Y.; Zhou, L.; Li, X.; Qian, R.; Wang, R.; Zhao, J.; Lou, K.; Wang, W. Enzymatic Cleavage and Subsequent Facile Intramolecular Transcyclization for in Situ Fluorescence Detection of γ-Glutamyltranspetidase Activities. *Anal. Chem.* **2016**, *88* (22), 10816−10820.
(43) Han, C.; Sun, S.-B.; Ji, X.; Wang, J.-Y. Recent advances in 1,8-naphthalimide-based responsive small-molecule fluorescent probes with a modified C4 position for the detection of biomolecules. *TrAC Trends in Analytical Chemistry* **2023**, *167*, 117242.
(44) Zhang, R.; Yuan, J. Responsive Metal Complex Probes for Time-Gated Luminescence Biosensing and Imaging. *Acc. Chem. Res.* **2020**, *53* (7), 1316−1329.
(45) Zhao, W.; Zhao, Y.; Wang, Q.; Liu, T.; Sun, J.; Zhang, R. Remote Light-Responsive Nanocarriers for Controlled Drug Delivery: Advances and Perspectives. *Small* **2019**, *15* (45), 1903060.
(46) Li, H.; Yao, Q.; Xu, F.; Xu, N.; Sun, W.; Long, S.; Du, J.; Fan, J.; Wang, J.; Peng, X. Lighting-Up Tumor for Assisting Resection via Spraying NIR Fluorescent Probe of γ-Glutamyltranspeptidas. *Frontiers in Chemistry* **2018**, *6*, 485.
(47) He, N.; Wang, Y.; Huang, Y.; Wang, X.; Chen, L.; Lv, C. A near-infrared fluorescent probe for evaluating glutamyl transpeptidase fluctuation in idiopathic pulmonary fibrosis cell and mice models. *Sens. Actuators, B* **2020**, *322*, 128565.
(48) Tian, L.; Feng, H.; Dai, Z.; Zhang, R. Resorufin-based responsive probes for fluorescence and colorimetric analysis. *J. Mater. Chem. B* **2021**, *9* (1), 53−79.
(49) Li, L.; Shi, W.; Wu, X.; Gong, Q.; Li, X.; Ma, H. Monitoring γ-glutamyl transpeptidase activity and evaluating its inhibitors by a water-soluble near-infrared fluorescent probe. *Biosens. Bioelectron.* **2016**, *81*, 395−400.
(50) Wu, M.; Niu, X.; Zhang, R.; Ping Xu, Z. Two-dimensional nanomaterials for tumor microenvironment modulation and anti-cancer therapy. *Adv. Drug Delivery Rev.* **2022**, *187*, 114360.
(51) Luo, Z.; Feng, L.; An, R.; Duan, G.; Yan, R.; Shi, H.; He, J.; Zhou, Z.; Ji, C.; Chen, H.-Y.; Ye, D. Activatable Near-Infrared Probe for Fluorescence Imaging of γ-Glutamyl Transpeptidase in Tumor Cells and In Vivo. *Chem. Eur. J.* **2017**, *23* (59), 14778−14785.
(52) Luo, Z.; Huang, Z.; Li, K.; Sun, Y.; Lin, J.; Ye, D.; Chen, H.-Y. Targeted Delivery of a γ-Glutamyl Transpeptidase Activatable Near-Infrared-Fluorescent Probe for Selective Cancer Imaging. *Anal. Chem.* **2018**, *90* (4), 2875−2883.
(53) Li, Y.; Xue, C.; Fang, Z.; Xu, W.; Xie, H. In Vivo Visualization of γ-Glutamyl Transpeptidase Activity with an Activatable Self-Immobilizing Near-Infrared Probe. *Anal. Chem.* **2020**, *92* (22), 15017−15024.
(54) Li, L.; Shi, W.; Wu, X.; Li, X.; Ma, H. In vivo tumor imaging by a γ-glutamyl transpeptidase-activatable near-infrared fluorescent probe. *Anal. Bioanal. Chem.* **2018**, *410* (26), 6771−6777.
(55) Liu, H.; Liu, F.; Wang, F.; Yu, R.-Q.; Jiang, J.-H. A novel mitochondrial-targeting near-infrared fluorescent probe for imaging γ-glutamyl transpeptidase activity in living cells. *Analyst* **2018**, *143* (22), 5530−5535.
(56) Koide, Y.; Urano, Y.; Hanaoka, K.; Piao, W.; Kusakabe, M.; Saito, N.; Terai, T.; Okabe, T.; Nagano, T. Development of NIR Fluorescent Dyes Based on Si−rhodamine for in Vivo Imaging. *J. Am. Chem. Soc.* **2012**, *134* (11), 5029−5031.
(57) Egawa, T.; Hanaoka, K.; Koide, Y.; Ujita, S.; Takahashi, N.; Ikegaya, Y.; Matsuki, N.; Terai, T.; Ueno, T.; Komatsu, T.; Nagano, T. Development of a Far-Red to Near-Infrared Fluorescence Probe for Calcium Ion and its Application to Multicolor Neuronal Imaging. *J. Am. Chem. Soc.* **2011**, *133* (36), 14157−14159.
(58) Koide, Y.; Urano, Y.; Hanaoka, K.; Terai, T.; Nagano, T. Development of an Si-Rhodamine-Based Far-Red to Near-Infrared Fluorescence Probe Selective for Hypochlorous Acid and Its Applications for Biological Imaging. *J. Am. Chem. Soc.* **2011**, *133* (15), 5680−5682.
(59) Li, M.; Wang, C.; Wang, T.; Fan, M.; Wang, N.; Ma, D.; Hu, T.; Cui, X. Asymmetric Si-rhodamine scaffolds: rational design of pH-durable protease-activated NIR probes in vivo. *Chem. Commun.* **2020**, *56* (16), 2455−2458.
(60) Zhang, L.-N.; Zhang, H.; Chen, S.-Y.; Liu, Y.-Z.; Yang, X.-H.; Xiang, F.-F.; Liu, Y.-H.; Li, K.; Yu, X.-Q. γ-Glutamyltranspeptidase and pH based "AND" logic gate fluorescent probe for orthotopic breast tumor imaging. *Chem. Commun.* **2023**, *59* (19), 2795−2798.
(61) Lee, H. W.; Juvekar, V.; Lee, D. J.; Kim, H. M. Recent advances in organelle-specific two-photon small-molecule fluorescent probes for bioanalysis in live tissues. *TrAC Trends in Analytical Chemistry* **2023**, *165*, 117128.
(62) Zhang, F.; Liang, X.; Zhang, W.; Wang, Y.-L.; Wang, H.; Mohammed, Y. H.; Song, B.; Zhang, R.; Yuan, J. A unique iridium(III) complex-based chemosensor for multi-signal detection

and multi-channel imaging of hypochlorous acid in liver injury. *Biosens. Bioelectron.* **2017**, *87*, 1005−1011.
(63) Wang, H.; Zhang, R.; Bridle, K. R.; Jayachandran, A.; Thomas, J. A.; Zhang, W.; Yuan, J.; Xu, Z. P.; Crawford, D. H. G.; Liang, X.; Liu, X.; Roberts, M. S. Two-photon dual imaging platform for in vivo monitoring cellular oxidative stress in liver injury. *Sci. Rep.* **2017**, *7* (1), 45374.
(64) Du, W.; Shao, T.; Wang, L.; Qin, W.; Fang, Z.; Fang, B.; Li, J.; Peng, B.; Wu, Q.; Liu, J.; Li, L. Two-photon fluorogenic probe off γ-glutamyl transpeptidase for cancer cells identification with simultaneous oxidative stress monitoring. *Dyes Pigm.* **2022**, *200*, 110155.
(65) Huo, R.; Zheng, X.; Liu, W.; Zhang, L.; Wu, J.; Li, F.; Zhang, W.; Lee, C.-S.; Wang, P. A two-photon fluorescent probe for sensitive detection and imaging of γ-glutamyl transpeptidase. *Chem. Commun.* **2020**, *56* (74), 10902−10905.
(66) Park, S.-H.; Kwon, N.; Lee, J.-H.; Yoon, J.; Shin, I. Synthetic ratiometric fluorescent probes for detection of ions. *Chem. Soc. Rev.* **2020**, *49* (1), 143−179.
(67) Lee, M. H.; Kim, J. S.; Sessler, J. L. Small molecule-based ratiometric fluorescence probes for cations, anions, and biomolecules. *Chem. Soc. Rev.* **2015**, *44* (13), 4185−4191.
(68) Chen, C.; Tian, R.; Zeng, Y.; Chu, C.; Liu, G. Activatable Fluorescence Probes for "Turn-On" and Ratiometric Biosensing and Bioimaging: From NIR-I to NIR-II. *Bioconjugate Chem.* **2020**, *31* (2), 276−292.
(69) Wang, S.; Liu, W.; Zheng, X.; Ren, H.; Wu, J.; Li, F.; Wang, P. A ratiometric fluorescent probe for detection of γ-glutamyl transpeptidase in blood serum and living cells. *Spectrochimica Acta Part A: Molecular and Biomolecular Spectroscopy* **2022**, *278*, 121325.
(70) Bai, B.; Yan, C.; Zhang, Y.; Guo, Z.; Zhu, W.-H. Dual-channel near-infrared fluorescent probe for real-time tracking of endogenous γ-glutamyl transpeptidase activity. *Chem. Commun.* **2018**, *54* (87), 12393−12396.
(71) Yang, L.; Xu, Y.; Dong, J.; Lu, Y.; Zhu, H.-L.; Li, Z. Imaging of a novel ratio γ-glutamyl transpeptidase fluorescent probe in living cells and biopsies. *Talanta* **2023**, *259*, 124504.
(72) Park, Y.; Ryu, Y.-M.; Wang, T.; Jung, Y.; Kim, S.; Hwang, S.; Park, J.; Bae, D.-J.; Kim, J.; Moon, H.; Lim, H.-S.; Kim, S.-Y.; Chung, E.; Kim, K. H.; Kim, S.; Myung, S.-J. Colorectal Cancer Diagnosis Using Enzyme-Sensitive Ratiometric Fluorescence Dye and Antibody−Quantum Dot Conjugates for Multiplexed Detection. *Adv. Funct. Mater.* **2018**, *28* (4), 1703450.
(73) Zhang, H.; Wang, K.; Xuan, X.; Lv, Q.; Nie, Y.; Guo, H. Cancer cell-targeted two-photon fluorescence probe for the real-time ratiometric imaging of DNA damage. *Chem. Commun.* **2016**, *52* (37), 6308−6311.
(74) Reo, Y. J.; Jun, Y. W.; Sarkar, S.; Dai, M.; Ahn, K. H. Ratiometric Imaging of γ-Glutamyl Transpeptidase Unperturbed by pH, Polarity, and Viscosity Changes: A Benzocoumarin-Based Two-Photon Fluorescent Probe. *Anal. Chem.* **2019**, *91* (21), 14101−14108.
(75) Reo, Y. J.; Dai, M.; Yang, Y. J.; Ahn, K. H. Cell-Membrane-Localizing, Two-Photon Probe for Ratiometric Imaging of γ-Glutamyl Transpeptidase in Cancerous Cells and Tissues. *Anal. Chem.* **2020**, *92* (18), 12678−12685.
(76) Liu, C.; Gao, X.; Yuan, J.; Zhang, R. Advances in the development of fluorescence probes for cell plasma membrane imaging. *TrAC Trends in Analytical Chemistry* **2020**, *133*, 116092.
(77) Kim, Y. J.; Park, S. J.; Lim, C. S.; Lee, D. J.; Noh, C.-K.; Lee, K.; Shin, S. J.; Kim, H. M. Ratiometric Detection of γ-Glutamyltransferase in Human Colon Cancer Tissues Using a Two-Photon Probe. *Anal. Chem.* **2019**, *91* (14), 9246−9250.
(78) Shi, B.; Zhang, Z.; Jin, Q.; Wang, Z.; Tang, J.; Xu, G.; Zhu, T.; Gong, X.; Tang, X.; Zhao, C. Selective tracking of ovarian-cancer-specific γ-glutamyltranspeptidase using a ratiometric two-photon fluorescent probe. *J. Mater. Chem. B* **2018**, *6* (45), 7439−7443.
(79) Zhang, R.; Song, B.; Yuan, J. Bioanalytical methods for hypochlorous acid detection: Recent advances and challenges. *TrAC Trends in Analytical Chemistry* **2018**, *99*, 1−33.
(80) Niu, J.; Wang, X.; Lv, J.; Li, Y.; Tang, B. Luminescent nanoprobes for in-vivo bioimaging. *TrAC Trends in Analytical Chemistry* **2014**, *58*, 112−119.
(81) Liu, Y.; Feng, B.; Cao, X.; Tang, G.; Liu, H.; Chen, F.; Liu, M.; Chen, Q.; Yuan, K.; Gu, Y.; Feng, X.; Zeng, W. A novel "AIE + ESIPT" near-infrared nanoprobe for the imaging of γ-glutamyl transpeptidase in living cells and the application in precision medicine. *Analyst* **2019**, *144* (17), 5136−5142.
(82) Wang, H.; Su, W.; Tan, M. Endogenous Fluorescence Carbon Dots Derived from Food Items. *Innovation* **2020**, *1* (1), 100009.
(83) Tong, X.; Li, T.; Long, R.; Guo, Y.; Wu, L.; Shi, S. Determination of the activity of γ-glutamyl transpeptidase and of its inhibitors by using the inner filter effect on the fluorescence of nitrogen-doped carbon dots. *Microchimica Acta* **2020**, *187* (3), 182.
(84) Cui, Y.; Zhang, L.; Shi, B.; Chen, S.; Zhao, S. Facile preparation of near-infrared fluorescent probes for highly sensitive detection of γ-glutamyl transpeptidase and evaluation of inhibitors. *Sens. Actuators, B* **2021**, *344*, 130080.
(85) Tong, X.; Zhu, Y.; Tong, C.; Shi, S.; Long, R.; Guo, Y. Simultaneous sensing γ-glutamyl transpeptidase and alkaline phosphatase by robust dual-emission carbon dots. *Anal. Chim. Acta* **2021**, *1178*, 338829.
(86) Lin, Y.; Gao, Y.; Ma, Z.; Jiang, T.; Zhou, X.; Li, Z.; Qin, X.; Huang, Y.; Du, L.; Li, M. Bioluminescence probe for γ-glutamyl transpeptidase detection in vivo. *Bioorg. Med. Chem.* **2018**, *26* (1), 134−140.
(87) An, R.; Wei, S.; Huang, Z.; Liu, F.; Ye, D. An Activatable Chemiluminescent Probe for Sensitive Detection of γ-Glutamyl Transpeptidase Activity in Vivo. *Anal. Chem.* **2019**, *91* (21), 13639−13646.
(88) Miao, M.; Miao, J.; Zhang, Y.; Zhang, J.; She, M.; Zhao, M.; Miao, Q.; Yang, L.; Zhou, K.; Li, Q. An activatable near-infrared molecular reporter for fluoro-photoacoustic imaging of liver fibrosis. *Biosens. Bioelectron.* **2023**, *235*, 115399.
(89) Jiang, L.; Guo, D.; Wang, L.; Chang, S.; Li, J.-B.; Zhan, D.-S.; Fodjo, E. K.; Gu, H.-X.; Li, D.-W. Sensitive and selective SERS probe for detecting the activity of γ-glutamyl transpeptidase in serum. *Anal. Chim. Acta* **2020**, *1099*, 119−125.
(90) Zhang, Y.; Zhang, G.; Yang, P.; Moosa, B.; Khashab, N. M. Self-Immolative Fluorescent and Raman Probe for Real-Time Imaging and Quantification of γ-Glutamyl Transpeptidase in Living Cells. *ACS Appl. Mater. Interfaces* **2019**, *11* (31), 27529−27535.
(91) Ye, S.; Wang, S.; Gao, D.; Li, K.; Liu, Q.; Feng, B.; Qiu, L.; Lin, J. A New γ-Glutamyltranspeptidase-Based Intracellular Self-Assembly of Fluorine-18 Labeled Probe for Enhancing PET Imaging in Tumors. *Bioconjugate Chem.* **2020**, *31* (2), 174−181.
(92) Sidiq, S.; Kumar, R. R.; Passi, N. D.; Dhawan, D. K.; Shukla, J.; Mittal, B. R.; Chadha, V. D. Evaluation of 99mTc-labeled glutathione as a colon cancer targeting probe. *Journal of Radioanalytical and Nuclear Chemistry* **2021**, *327* (2), 673−689.
(93) Wang, X.; Gao, D.; Lu, C.; Xie, M.; Lin, J.; Qiu, L. Optimized molecular design of PET probe for the visualization of γ-glutamyltranspeptidase activity in tumors. *New J. Chem.* **2022**, *46* (21), 10219−10228.
(94) Nishihara, T.; Yoshihara, H. A. I.; Nonaka, H.; Takakusagi, Y.; Hyodo, F.; Ichikawa, K.; Can, E.; Bastiaansen, J. A. M.; Takado, Y.; Comment, A.; Sando, S. Direct Monitoring of γ-Glutamyl Transpeptidase Activity In Vivo Using a Hyperpolarized 13C-Labeled Molecular Probe. *Angew. Chem., Int. Ed.* **2016**, *55* (36), 10626−10629.
(95) Hai, Z.; Ni, Y.; Saimi, D.; Yang, H.; Tong, H.; Zhong, K.; Liang, G. γ-Glutamyltranspeptidase-Triggered Intracellular Gadolinium Nanoparticle Formation Enhances the T2-Weighted MR Contrast of Tumor. *Nano Lett.* **2019**, *19* (4), 2428−2433.
(96) Rathbun, C. M.; Prescher, J. A. Bioluminescent Probes for Imaging Biology beyond the Culture Dish. *Biochemistry* **2017**, *56* (39), 5178−5184.

https://doi.org/10.1021/acsmeasuresciau.3c00045
ACS Meas. Sci. Au 2024, 4, 54−75

(97) Yao, Z.; Zhang, B. S.; Prescher, J. A. Advances in bioluminescence imaging: new probes from old recipes. *Curr. Opin. Chem. Biol.* **2018**, *45*, 148−156.
(98) Li, J.; Chen, L.; Du, L.; Li, M. Cage the firefly luciferin! − a strategy for developing bioluminescent probes. *Chem. Soc. Rev.* **2013**, *42* (2), 662−676.
(99) Wang, Z.; Huang, J.; Huang, J.; Yu, B.; Pu, K.; Xu, F.-J. Chemiluminescence: From mechanism to applications in biological imaging and therapy. *Aggregate* **2021**, *2* (6), e140.
(100) Li, X.; Yin, C.; Liew, S. S.; Lee, C.-S.; Pu, K. Organic Semiconducting Luminophores for Near-Infrared Afterglow, Chemiluminescence, and Bioluminescence Imaging. *Adv. Funct. Mater.* **2021**, *31* (46), 2106154.
(101) Rajendran, P.; Sharma, A.; Pramanik, M. Photoacoustic imaging aided with deep learning: a review. *Biomedical Engineering Letters* **2022**, *12* (2), 155−173.
(102) He, C.; Zhu, J.; Zhang, H.; Qiao, R.; Zhang, R. Photoacoustic Imaging Probes for Theranostic Applications. *Biosensors* **2022**, *12* (11), 947.
(103) Tavakkoli Yaraki, M.; Tukova, A.; Wang, Y. Emerging SERS biosensors for the analysis of cells and extracellular vesicles. *Nanoscale* **2022**, *14* (41), 15242−15268.
(104) Shoup, D. N.; Scarpitti, B. T.; Schultz, Z. D. A Wide-Field Imaging Approach for Simultaneous Super-Resolution Surface-Enhanced Raman Scattering Bioimaging and Spectroscopy. *ACS Measurement Science Au* **2022**, *2* (4), 332−341.
(105) Han, X. X.; Rodriguez, R. S.; Haynes, C. L.; Ozaki, Y.; Zhao, B. Surface-enhanced Raman spectroscopy. *Nature Reviews Methods Primers* **2021**, *1*, 87.
(106) Gawne, P. J.; Man, F.; Blower, P. J.; de Rosales, R. T. M. Direct Cell Radiolabeling for in Vivo Cell Tracking with PET and SPECT Imaging. *Chem. Rev.* **2022**, *122* (11), 10266−10318.
(107) Meng, Q.; Wu, M.; Shang, Z.; Zhang, Z.; Zhang, R. Responsive gadolinium(III) complex-based small molecule magnetic resonance imaging probes: Design, mechanism and application. *Coord. Chem. Rev.* **2022**, *457*, 214398.
(108) Fujikawa, Y.; Mori, M.; Tsukada, M.; Miyahara, S.; Sato-Fukushima, H.; Watanabe, E.; Murakami-Tonami, Y.; Inoue, H. Pi-Class Glutathione S-transferase (GSTP1)-Selective Fluorescent Probes for Multicolour Imaging with Various Cancer-Associated Enzymes. *ChemBioChem.* **2022**, *23* (21), e202200443.
(109) Kubo, H.; Hanaoka, K.; Kuriki, Y.; Komatsu, T.; Ueno, T.; Kojima, R.; Kamiya, M.; Murayama, Y.; Otsuji, E.; Urano, Y. Rapid detection of metastatic lymph nodes of colorectal cancer with a gamma-glutamyl transpeptidase-activatable fluorescence probe. *Sci. Rep.* **2018**, *8* (1), 17781.
(110) Yamashita, S.; Sakabe, M.; Ishizawa, T.; Hasegawa, K.; Urano, Y.; Kokudo, N. Visualization of the leakage of pancreatic juice using a chymotrypsin-activated fluorescent probe. *British Journal of Surgery* **2013**, *100* (9), 1220−1228.
(111) Sato, C.; Abe, S.; Saito, Y.; So Tsuruki, E.; Takamaru, H.; Makazu, M.; Sato, Y.; Sasaki, H.; Tanaka, H.; Ikezawa, N.; Yamada, M.; Sakamoto, T.; Nakajima, T.; Matsuda, T.; Kushima, R.; Kamiya, M.; Maeda, S.; Urano, Y. A Pilot Study of Fluorescent Imaging of Colorectal Tumors Using a γ-Glutamyl-Transpeptidase-Activatable Fluorescent Probe. *Digestion* **2015**, *91* (1), 70−76.
(112) Nakada, A.; Maruyama, T.; Kamiya, M.; Hanaoka, K.; Urano, Y. Rapid Visualization of Deeply Located Tumors In Vivo by Intravenous Administration of a γ-Glutamyltranspeptidase-Activated Fluorescent Probe. *Bioconjugate Chem.* **2022**, *33* (3), 523−529.
(113) Hino, H.; Kamiya, M.; Kitano, K.; Mizuno, K.; Tanaka, S.; Nishiyama, N.; Kataoka, K.; Urano, Y.; Nakajima, J. Rapid Cancer Fluorescence Imaging Using A γ-Glutamyltranspeptidase-Specific Probe For Primary Lung Cancer. *Translational Oncology* **2016**, *9* (3), 203−210.
(114) Yamada, K.; Takata, T.; Iyama, T.; Hamada, S.; Mae, Y.; Sugihara, T.; Isomoto, H. Fluorescence Imaging Using Enzyme-Activatable Probes for Detecting Diabetic Kidney Disease and Glomerular Diseases. *International Journal of Molecular Sciences* **2022**, *23* (15), 8150.
(115) Shibayama, K.; Kamachi, K.; Nagata, N.; Yagi, T.; Nada, T.; Doi, Y.; Shibata, N.; Yokoyama, K.; Yamane, K.; Kato, H.; Iinuma, Y.; Arakawa, Y. A novel apoptosis-inducing protein from Helicobacter pylori. *Mol. Microbiol.* **2003**, *47* (2), 443−451.
(116) Akashi, T.; Isomoto, H.; Matsushima, K.; Kamiya, M.; Kanda, T.; Nakano, M.; Onoyama, T.; Fujii, M.; Akada, J.; Akazawa, Y.; Ohnita, K.; Takeshima, F.; Nakao, K.; Urano, Y. A novel method for rapid detection of a Helicobacter pylori infection using a γ-glutamyltranspeptidase-activatable fluorescent probe. *Sci. Rep.* **2019**, *9* (1), 9467.
(117) Wang, C.; Tian, Z.; Wang, Y.; Zhang, M.; Zhang, B.; Feng, L.; Tian, X.; Huang, H.; Cui, J.; Ma, X. An enzyme-activated NIR fluorescent probe for detecting bacterial glutamyltranspeptidase (γ-GT) and high-throughput screening of its inhibitors. *Sens. Actuators, B* **2021**, *329*, 129225.
(118) Liu, T.; Yan, Q.-L.; Feng, L.; Ma, X.-C.; Tian, X.-G.; Yu, Z.-L.; Ning, J.; Huo, X.-K.; Sun, C.-P.; Wang, C.; Cui, J.-N. Isolation of γ-Glutamyl-Transferase Rich-Bacteria from Mouse Gut by a Near-Infrared Fluorescent Probe with Large Stokes Shift. *Anal. Chem.* **2018**, *90* (16), 9921−9928.
(119) Xue, H.; Lu, J.; Yan, H.; Huang, J.; Luo, H.-B.; Wong, M. S.; Gao, Y.; Zhang, X.; Guo, L. γ-Glutamyl transpeptidase−activated indole-quinolinium based cyanine as a fluorescence turn-on nucleolus-targeting probe for cancer cell detection and inhibition. *Talanta* **2022**, *237*, 122898.
(120) Pham, T. C.; Nguyen, V.-N.; Choi, Y.; Lee, S.; Yoon, J. Recent Strategies to Develop Innovative Photosensitizers for Enhanced Photodynamic Therapy. *Chem. Rev.* **2021**, *121* (21), 13454−13619.
(121) Wu, M.; Yong, J.; Zhang, H.; Wang, Z.; Xu, Z. P.; Zhang, R. 2D Ultrathin Iron Doped Bismuth Oxychloride Nanosheets with Rich Oxygen Vacancies for Enhanced Sonodynamic Therapy. *Adv. Healthcare Mater.* **2023**, 2301497.
(122) Chiba, M.; Ichikawa, Y.; Kamiya, M.; Komatsu, T.; Ueno, T.; Hanaoka, K.; Nagano, T.; Lange, N.; Urano, Y. An Activatable Photosensitizer Targeted to γ-Glutamyltranspeptidase. *Angew. Chem., Int. Ed.* **2017**, *56* (35), 10418−10422.
(123) Mukaimine, A.; Hirayama, T.; Nagasawa, H. Asymmetric bismuth-rhodamines as an activatable fluorogenic photosensitizer. *Organic & Biomolecular Chemistry* **2021**, *19* (16), 3611−3619.
(124) Yang, Z.; Xu, W.; Wang, J.; Liu, L.; Chu, Y.; Wang, Y.; Hu, Y.; Yi, T.; Hua, J. Diketopyrrolopyrrole-based multifunctional ratiometric fluorescent probe and γ-glutamyltranspeptidase-triggered activatable photosensitizer for tumor therapy. *Journal of Materials Chemistry C* **2020**, *8* (24), 8183−8190.
(125) Li, J.; Wang, T.; Jiang, F.; Hong, Z.; Su, X.; Li, S.; Han, S. A fluorescence-activatable tumor-reporting probe for precise photodynamic therapy. *J. Mater. Chem. B* **2021**, *9* (29), 5829−5836.
(126) Li, X.; Lovell, J. F.; Yoon, J.; Chen, X. Clinical development and potential of photothermal and photodynamic therapies for cancer. *Nature Reviews Clinical Oncology* **2020**, *17* (11), 657−674.
(127) Overchuk, M.; Weersink, R. A.; Wilson, B. C.; Zheng, G. Photodynamic and Photothermal Therapies: Synergy Opportunities for Nanomedicine. *ACS Nano* **2023**, *17* (9), 7979−8003.
(128) Zhou, F.; Yang, S.; Zhao, C.; Liu, W.; Yao, X.; Yu, H.; Sun, X.; Liu, Y. γ-Glutamyl transpeptidase-activatable near-infrared nanoassembly for tumor fluorescence imaging-guided photothermal therapy. *Theranostics* **2021**, *11* (14), 7045−7056.

https://doi.org/10.1021/acsmeasuresciau.3c00045
ACS Meas. Sci. Au 2024, 4, 54−75